Coordination and Rupture of Methyl C(sp^3)−H Bonds in Osmium−Polyhydride Complexes with δ Agostic Interaction

Miguel Baya,[†,‡] Beatriz Eguillor,[†] Miguel A. Esteruelas,*[,†] Agustí Lledós,*[,‡] Montserrat Oliván,[†] and Enrique Oñate[†]

Departamento de Química Inorgánica, Instituto de Ciencia de Materiales de Aragón, Universidad de Zaragoza-CSIC, 50009 Zaragoza, Spain, and Unitat de Química Física, Edifici C.n, Universitat Autònoma de Barcelona, 08193 Bellaterra, Spain

Received May 22, 2007

The hexahydride complex $OsH_6(P^iPr_3)_2$ (**1**) reacts with 8-methylquinoline and 2-(dimethylamino)pyridine to give $OsH_3(CH_2C_9H_6N)(P^iPr_3)_2$ (**2**) and $OsH_3\{CH_2N(CH_3)$-*o*-$C_5H_4N\}(P^iPr_3)_2$ (**3**), respectively, as a result of the release of two hydrogen molecules of **1** and the C(sp^3)−H bond activation of a methyl group of the organic substrates. In solution the hydride ligands and the hydrogen atoms of the methylene group of **2** exchange their positions. The activation parameters for the process are $\Delta H^{\ddagger} = 18.9 \pm 0.1$ kcal·mol^{-1} and $\Delta S^{\ddagger} = 3 \pm 2$ eu. Treatment of **2** with HBF_4 affords the hydride-elongated dihydrogen derivative $[OsH(\eta^2\text{-}H_2)(CH_3C_9H_6N)(P^iPr_3)_2]BF_4$ (**6**), with the methyl group of the quinoline ligand coordinated in a η^3-H_2C fashion. The X-ray structure of **6** and the DFT optimization of the structure of the model cation $[OsH(\eta^2\text{-}H_2)(CH_4)(NH_3)(PMe_3)_2]^+$ prove that the methyl coordination in the δ agostic complex is similar to the methane coordination in the model compound. The reaction of **3** with HBF_4 leads to the cyclic carbene derivative $[OsH_3\{{=}CHN(CH_3)$-*o*-$C_5H_4N\}(P^iPr_3)_2]BF_4$ (**7**), as a result of the release of a hydrogen molecule and a C(sp^3)−H bond activation on the methylene group of **3**. The formation of **2**, **3**, **6**, and **7** has been analyzed by DFT calculations.

Introduction

Transition metal polyhydride complexes have long been known to be stereochemically nonrigid. They exhibit fluxional behavior with rapid permutation of the hydride ligands. After the discovery that hydrogen molecules can be present in the coordination sphere of a metal without cleavage of the hydrogen−hydrogen bond, dihydrogen ligands have proven to be key moieties to the site exchanges.[1]

The bonding interactions between the metal and the hydrogen molecule have been described in terms of donation from the filled σ-bonding orbital into an empty orbital of σ symmetry on the metal. This interaction is augmented by back-donation from filled metal orbitals of predominant d character to the σ^* orbital of the hydrogen molecule. Both interactions weaken and lengthen the hydrogen−hydrogen bond. In the limit of strong back-donation, bond cleavage to form two hydrides results.[2]

The interrelationships between activation of molecular hydrogen and other σ-bond molecules such as alkanes, in particular methane, are highly significant because their conversion is being pursued intensively.[3] Molecular hydrogen and methane have orbitals of reasonably similar shape, energy, and extent. The HOMO of methane is a t_2 C−H bonding orbital, with an experimental IE of 12.54 eV, whereas the molecular hydrogen σ orbital has an IE of 15.45 eV. The LUMO is the t_2 antibonding counterpart and lies at a similar energy to the σ^* orbital of molecular hydrogen.[4] In the case of hydrogen, the approach to the metal fragment is more attractive for a parallel arrangement due to the possibility of back-bonding from the metal to the σ^* orbital. However, for methane, the C−H parallel arrangement is disfavored by steric repulsion from the metal. Theoretical calculations show that an η^3-H_2C coordination should be the most stable.[5]

Great experimental attention has been devoted to the fate of an alkane molecule that approaches an unsaturated metal fragment. However, unfortunately, information on the nature of the primary adduct is still scarce, since saturated hydrocarbons are notoriously very poor ligands. Thus, not surprisingly, all

* Corresponding authors. E-mail: maester@unizar.es; agusti@klingon.uab.es.
† Universidad de Zaragoza-CSIC.
‡ Universitat Autònoma de Barcelona.

(1) (a) Moore, D. S.; Robinson, S. D. *Chem. Soc. Rev.* **1983**, *12*, 415. (b) Kubas, G. J. *Acc. Chem. Res.* **1988**, *21*, 120. (c) Jessop, P. G.; Morris, R. H. *Coord. Chem. Rev.* **1992**, *121*, 155. (d) Crabtree, R. H. *Angew. Chem., Int. Ed. Engl.* **1993**, *32*, 789. (e) Heinekey, D. M.; Oldham, W. J. *Chem. Rev.* **1993**, *93*, 913. (f) Gusev, D. G.; Berke, H. *Chem. Ber.* **1996**, *129*, 1143. (g) Jia, G.; Lau, C.-P. *Coord. Chem. Rev.* **1999**, *190*−*192*, 83. (h) Maseras, F.; Lledos, A.; Clot, E.; Eisenstein, O. *Chem. Rev.* **2000**, *100*, 601. (i) Heinekey, D. M.; Lledós, A.; Lluch, J. M. *Chem. Soc. Rev.* **2004**, *33*, 175. (j) Perutz, R. N.; Sabo-Etienne, S. *Angew. Chem., Int. Ed.* **2007**, *46*, 2578. (k) Brookhart, M.; Green, M. L. H.; Parkin, G. *PNAS* **2007**, *104*, 6908.

(2) Kubas, G. J. *Metal Dihydrogen and σ-Bond Complexes*; Kluwer Academic/Plenum Publishers: New York, 2001.

(3) (a) Ryabov, A. D. *Chem. Rev.* **1990**, *90*, 403. (b) Arndtsen, B. A.; Bergman, R. G. *Science* **1995**, *270*, 1970. (c) Shilov, A. E.; Shul'pin, G. B. *Chem. Rev.* **1997**, *97*, 2879. (d) Stahl, S. S.; Labinger, J. A.; Bercaw, J. E. *Angew. Chem., Int. Ed.* **1998**, *37*, 2180. (e) Chen, H.; Schlecht, S.; Semple, T. C.; Hartwig, J. F. *Science* **2000**, *287*, 1995. (f) Crabtree, R. H. *J. Chem. Soc., Dalton Trans.* **2001**, 2437. (g) Labinger, J. A.; Bercaw, J. E. *Nature* **2002**, *417*, 507. (h) Periana, R. A.; Mironov, O.; Taube, D.; Bhalla, G.; Jones, C. J. *Science* **2003**, *301*, 814. (i) Crabtree, R. H. *J. Organomet. Chem.* **2004**, *689*, 4083. (j) Lersch, M.; Tilset, M. *Chem. Rev.* **2005**, *105*, 2471.

(4) Hall, C.; Perutz, R. N. *Chem. Rev.* **1996**, *96*, 3125.

10.1021/om700509d CCC: $37.00
Publication on Web 09/15/2007

the alkane complexes detected so far are unstable at room temperature and their detection has required specialized methods.[4,6]

Hydrogen exchanges between hydride and alkyl ligands in monohydride metal−alkyl complexes have also been reported in support of alkane σ complexes.[7] On the other hand, in contrast to the hydride−dihydrogen site exchange, hydrogen exchanges between alkyl groups and hydride and dihydrogen ligands in polyhydride compounds containing coordinated C(sp³)−H bonds have not been investigated.

The effective approach of an alkane fragment to a transition metal generally needs the assistance of a coordination auxiliary.[8] Following Kubas' opinion,[2] one could argue that an agostic complex involving intramolecular interaction rather external ligand binding should not be taken into account as a σ compound. However, it should be noted that for those interactions where the implied CH_3 group is connected to the metal center by two or more atoms the distinction is somewhat artificial.[9] In particular for δ-agostic complexes, Baratta, Mealli, and co-workers have elegantly demonstrated that the structural parameters involving the methyl groups and the metal center of complex $RuCl_2\{PPh_2(2,6\text{-}Me_2C_6H_3)\}_2$ are similar to those expected for the coordination of a methane molecule to the same metal skeleton.[10] The coordination of the pyridinic nitrogen atom of 8-methylquinoline and 2-dimethylaminopyridine to 14-valence-electron metal fragments should also afford δ-agostic compounds. However, those reported have been described as classical η^2-HC species.[11]

As a part of the work of our group on the chemistry of polyhydride− and dihydrogen−osmium complexes,[12] we have previously reported that complexes $OsH_6(P^iPr_3)_2$, $OsH_3(SnClPh_2)\{[\eta^2\text{-}CH_2{=}C(CH_3)]P^iPr_2\}(P^iPr_3)$, and $[OsH_2(\eta^5\text{-}C_5H_5)(\eta^2\text{-}H_2)(P^iPr_3)]BF_4$ activate C(sp²)−H bonds of amines,[13] ketones,[14] and aldehydes.[15] Complex $OsH_6(P^iPr_3)_2$ is also capable of producing a triple C(sp³)−H bond activation of the cyclohexyl group of cyclohexylmethyl ketone to afford the trihydride−osmafurane $OsH_3\{C_6H_8C(O)CH_3\}(P^iPr_3)_2$.[16] These results and our interest in learning to functionalize the C(sp³)−H bond[17] prompted us to investigate the behavior of the methyl groups of 8-methylquinoline and 2-(dimethylamino)pyridine in the presence of the hexahydride complex $OsH_6(P^iPr_3)_2$.

In this paper, we report the following: (i) the C(sp³)−H bond activation of the methyl groups of both organic substrates and the hydrogen exchange processes in the resulting species, (ii) a theoretical study on the C(sp³)−H bond activation reactions, (iii) the coordination of the methyl group of 8-methylquinoline and a second C(sp³)−H bond activation of the activated methyl group of 2-(dimethylamino)pyridine, as a result of the protonation of the resulting species from the first C(sp³)−H bond

(5) (a) Koga, N.; Morokuma, K. *J. Phys. Chem.* **1990**, *94*, 5454. (b) Re, N.; Rosi, M.; Sgamellotti, A.; Floriani, C.; Guest, M. F. *J. Chem. Soc., Dalton Trans.* **1992**, 1821. (c) Cundari, T. R. *J. Am. Chem. Soc.* **1994**, *116*, 340. (d) Margl, P.; Ziegler, T.; Blöchl, P. E. *J. Am. Chem. Soc.* **1995**, *117*, 12625. (e) Martin, R. L. *J. Am. Chem. Soc.* **1999**, *121*, 9459. (f) Heiberg, H.; Johansson, L.; Gropen, O.; Ryan, O. B.; Swang, O.; Tilset, M. *J. Am. Chem. Soc.* **2000**, *122*, 10831. (g) Szilagyi, R. K.; Musaev, D. G.; Morokuma, K. *Organometallics* **2002**, *21*, 555.

(6) (a) Sun, X.-Z.; Grills, D. C.; Nikiforov, S. M.; Poliakoff, M.; George, M. W. *J. Am. Chem. Soc.* **1997**, *119*, 7521. (b) Geftakis, S.; Ball, G. E. *J. Am. Chem. Soc.* **1998**, *120*, 9953. (c) Childs, G. I.; Grills, D. C.; Sun, X. Z.; George, M. W. *Pure Appl. Chem.* **2001**, *73*, 443. (d) Krishnan, R.; Schultz, R. H. *Organometallics* **2001**, *20*, 3314. (e) Castro-Rodríguez, I.; Nakai, H.; Gantzel, P.; Zakharov, L. N.; Rheingold, A. L.; Meyer, K. *J. Am. Chem. Soc.* **2003**, *125*, 15734. (f) Lawes, D. J.; Geftakis, S.; Ball, G. E. *J. Am. Chem. Soc.* **2005**, *127*, 4134.

(7) (a) Wang, C.; Ziller, J. W.; Flood, T. C. *J. Am. Chem. Soc.* **1995**, *117*, 1647. (b) Stahl, S. S.; Labinger, J. A.; Bercaw, J. E. *J. Am. Chem. Soc.* **1996**, *118*, 5961. (c) Gross, C. L.; Girolami, G. S. *J. Am. Chem. Soc.* **1998**, *120*, 6605. (d) Wick, D. D.; Reynolds, K. A.; Jones, W. D. *J. Am. Chem. Soc.* **1999**, *121*, 3974. (e) Northcutt, T. O.; Wick, D. D.; Vetter, A. J.; Jones, W. D. *J. Am. Chem. Soc.* **2001**, *123*, 7257. (f) Lo, H. C.; Haskel, A.; Kapon, M.; Keinan, E. *J. Am. Chem. Soc.* **2002**, *124*, 3226. (g) Jones, W. D. *Acc. Chem. Res.* **2003**, *36*, 140. (h) Prokopchuk, E. M.; Puddephatt, R. J. *Organometallics* **2003**, *22*, 787. (i) Ng, S. M.; Lam, W. H.; Mak, C. C.; Tsang, C. W.; Jia, G.; Lin, Z.; Lau, C. P. *Organometallics* **2003**, *22*, 641.

(8) (a) Bennett, M. A.; McMahon, I. J.; Pelling, S.; Robertson, G. B.; Wickramasinghe, W. A. *Organometallics* **1985**, *4*, 754. (b) Huang, D. J.; Huffman, J. C.; Bollinger, J. C.; Eisenstein, O.; Caulton, K. G. *J. Am. Chem. Soc.* **1997**, *119*, 7398. (c) Huang, D. J.; Streib, W. E.; Eisenstein, O.; Caulton, K. G. *Angew. Chem., Int. Ed. Engl.* **1997**, *36*, 2004. (d) Huang, D.; Streib, W. E.; Bollinger, J. C.; Caulton, K. G.; Winter, R. F.; Scheiring, T. *J. Am. Chem. Soc.* **1999**, *121*, 8087. (e) Takahashi, Y.; Hikichi, S.; Akita, M.; Moro-oka, Y. *Organometallics* **1999**, *18*, 2571. (f) Cooper, A. C.; Clot, E.; Huffman, J. C.; Streib, W. E.; Maseras, F.; Eisenstein, O.; Caulton, K. G. *J. Am. Chem. Soc.* **1999**, *121*, 97. (g) Baratta, W.; Herdtweck, E.; Rigo, P. *Angew. Chem., Int. Ed.* **1999**, *38*, 1629. (h) Wen, T. B.; Zhou, Z. Y.; Lau, C.-P.; Jia, G. *Organometallics* **2000**, *19*, 3466. (i) Urtel, H.; Meier, C.; Eisenträger, F.; Rominger, F.; Joschek, J. P.; Hofmann, P. *Angew. Chem., Int. Ed.* **2001**, *40*, 781. (j) Clot, E.; Eisenstein, O.; Dubé, T.; Faller, J. W.; Crabtree, R. H. *Organometallics* **2002**, *21*, 575. (k) Baratta, W.; Da Ros, P.; Del Zotto, A.; Sechi, A.; Zangrando, E.; Rigo, P. *Angew. Chem., Int. Ed.* **2004**, *43*, 3584. (l) Abdur-Rashid, K.; Fedorkiw, T.; Lough, A. J.; Morris, R. H. *Organometallics* **2004**, *23*, 86. (m) Baratta, W.; Del Zotto, A.; Esposito, G.; Sechi, A.; Toniutti, M.; Zangrando, E.; Rigo, P. *Organometallics* **2004**, *23*, 6264. (n) Burling, S.; Kociok-Köhn, G.; Mahon, M. F.; Whittlesey, M. K.; Williams, J. M. J. *Organometallics* **2005**, *24*, 5868. (o) Scott, N. M.; Pons, V.; Stevens, E. D.; Heinekey, D. M.; Nolan, S. P. *Angew. Chem., Int. Ed.* **2005**, *44*, 2512. (p) Scott, N. M.; Dorta, R.; Stevens, E. D.; Correa, A.; Cavallo, L.; Nolan, S. P. *J. Am. Chem. Soc.* **2005**, *127*, 3516. (q) Lewis, J. C.; Wu, J.; Bergman, R. G.; Ellman, J. A. *Organometallics* **2005**, *24*, 5737. (r) Brayshaw, S. K.; Green, J. C.; Kociok-Köhn, G.; Sceats, E. L.; Weller, A. S. *Angew. Chem., Int. Ed.* **2006**, *45*, 452.

(9) Clot, E.; Eisenstein, O. *Struct. Bonding* **2004**, *113*, 1.

(10) Baratta, W.; Mealli, C.; Herdtweck, E.; Ienco, A.; Mason, S. A.; Rigo, P. *J. Am. Chem. Soc.* **2004**, *126*, 5549.

(11) (a) Crabtree, R. H.; Holt, E. M.; Lavin, M.; Morehouse, S. M. *Inorg. Chem.* **1985**, *24*, 1986. (b) Neve, F.; Ghedini, M.; De Munno, G.; Crispini, A. *Organometallics* **1991**, *10*, 1143. (c) Neve, F.; Ghedini, M.; Crispini, A. *Organometallics* **1992**, *11*, 3324. (d) Holcomb, H. L.; Nakanishi, S.; Flood, T. C. *Organometallics* **1996**, *15*, 4228.

(12) For some recent examples see: (a) Esteruelas, M. A.; Lledós, A.; Martín, M.; Maseras, F.; Osés, R.; Ruiz, N.; Tomàs, J. *Organometallics* **2001**, *20*, 5297. (b) Esteruelas, M. A.; García-Yebra, C.; Oliván, M.; Oñate, E.; Tajada, M. A. *Organometallics* **2002**, *21*, 1311. (c) Barrio, P.; Esteruelas, M. A.; Oñate, E. *Organometallics* **2002**, *21*, 2491. (d) Esteruelas, M. A.; Lledós, A.; Maseras, F.; Oliván, M.; Oñate, E.; Tajada, M. A.; Tomas, J. *Organometallics* **2003**, *22*, 2087. (e) Barrio, P.; Esteruelas, M. A.; Oñate, E. *Organometallics* **2003**, *22*, 2472. (f) Barrio, P.; Esteruelas, M. A.; Oñate, E. *J. Am. Chem. Soc.* **2004**, *126*, 1946. (g) Esteruelas, M. A.; Lledos, A.; Maresca, O.; Oliván, M.; Oñate, E.; Tajada, M. A. *Organometallics* **2004**, *23*, 1453. (h) Barrio, P.; Esteruelas, M. A.; Lledós, A.; Oñate, E.; Tomàs, J. *Organometallics* **2004**, *23*, 3008. (i) Eguillor, B.; Esteruelas, M. A.; Oliván, M. *Organometallics* **2006**, *25*, 4691. (j) Esteruelas, M. A.; Fernández-Alvarez, F. J.; Oñate, E. *J. Am. Chem. Soc.* **2006**, *128*, 13044.

(13) (a) Barea, G.; Esteruelas, M. A.; Lledós, A.; López, A. M.; Oñate, E.; Tolosa, J. I. *Organometallics* **1998**, *17*, 4065. (b) Barrio, P.; Esteruelas, M. A.; Oñate, E. *Organometallics* **2004**, *23*, 3627.

(14) (a) Barrio, P.; Castarlenas, R.; Esteruelas, M. A.; Lledós, A.; Maseras, F.; Oñate, E.; Tomàs, J. *Organometallics* **2001**, *20*, 442. (b) Esteruelas, M. A.; Lledós, A.; Oliván, M.; Oñate, E.; Tajada, M. A.; Ujaque, G. *Organometallics* **2003**, *22*, 3753. (c) Eguillor, B.; Esteruelas, M. A.; Oliván, M.; Oñate, E. *Organometallics* **2005**, *24*, 1428. (d) Esteruelas, M. A.; Hernández, Y. A.; López, A. M.; Oliván, M.; Oñate, E. *Organometallics* **2005**, *24*, 5989.

(15) (a) Barrio, P.; Esteruelas, M. A.; Oñate, E. *Organometallics* **2004**, *23*, 1340. (b) Eguillor, B.; Esteruelas, M. A.; Oliván, M.; Oñate, E. *Organometallics* **2004**, *23*, 6015.

(16) Barrio, P.; Castarlenas, R.; Esteruelas, M. A.; Oñate, E. *Organometallics* **2001**, *20*, 2635.

(17) (a) Baya, M.; Buil, M. L.; Esteruelas, M. A.; Oñate, E. *Organometallics* **2004**, *23*, 1416. (b) Esteruelas, M. A.; González, A. I.; López, A. M.; Oñate, E. *Organometallics* **2004**, *23*, 4858. (c) Baya, M.; Esteruelas, M. A.; González, A. I.; López, A. M.; Oñate, E. *Organometallics* **2005**, *24*, 1225. (d) Baya, M.; Buil, M. L.; Esteruelas, M. A.; Oñate, E. *Organometallics* **2005**, *24*, 2030. (e) Baya, M.; Buil, M. L.; Esteruelas, M. A.; Oñate, E. *Organometallics* **2005**, *24*, 5180.

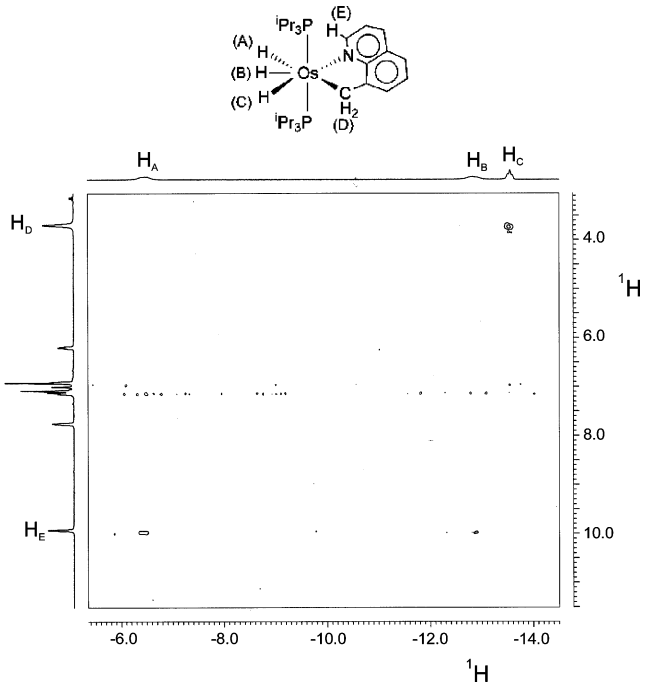

Figure 1. Partial view of the ^{1}H-NOESY (300 MHz, mixing time = 100 ms, toluene-d_8, 213 K) NMR spectrum of $OsH_3(CH_2C_9H_6N](P^iPr_3)_2$ (**2**).

activation, and (iv) a theoretical study analyzing the different behavior of related pyridine-based ligands after protonation.

Results and Discussion

1. C(sp^3)−H Bond Activation and Hydrogen Exchange Processes. Treatment under reflux of toluene solutions of the hexahydride complex $OsH_6(P^iPr_3)_2$ (**1**) with 1.5 equiv of 8-methylquinoline leads after 90 min to the trihydride derivative $OsH_3(CH_2C_9H_6N)(P^iPr_3)_2$ (**2**), as a result of the release of two hydrogen molecules of **1** and the C(sp^3)−H bond activation of the methyl substituent of the quinoline substrate. Complex **2** is isolated as a red solid in 97% yield, according to eq 1.

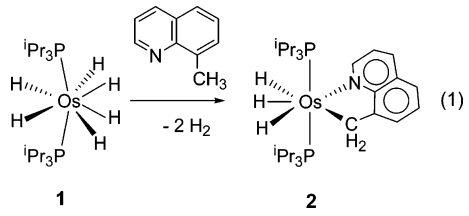

The ^{13}C{^{1}H}, ^{31}P{^{1}H}, and ^{1}H NMR spectra of **2** at 193 K in toluene-d_8 are consistent with the structure proposed in eq 1. In the ^{13}C{^{1}H} NMR spectrum, the methylene resonance of the heterometallacycle appears at 6.7 ppm, as a triplet with a C−P coupling constant of 5 Hz. In agreement with the mutually *trans* disposition of the phosphine ligands, the ^{31}P{^{1}H} spectrum contains a singlet at 23.1 ppm. As expected for the three inequivalent hydride ligands, the ^{1}H spectrum shows three hydride resonances at −6.35 (**A**), −12.75 (**B**), and −13.46 (**C**) ppm. The signal corresponding to the methylene protons (**D**) appears at 3.81 ppm, whereas that due to the α-proton of the quinoline group (**E**) is observed at 9.95 ppm. According to the NOESY spectrum shown in Figure 1, the trihydride signals **A**, **B**, and **C** correspond to the ligands *cis* to the nitrogen atom, central, and *cis* to the methylene group, respectively.

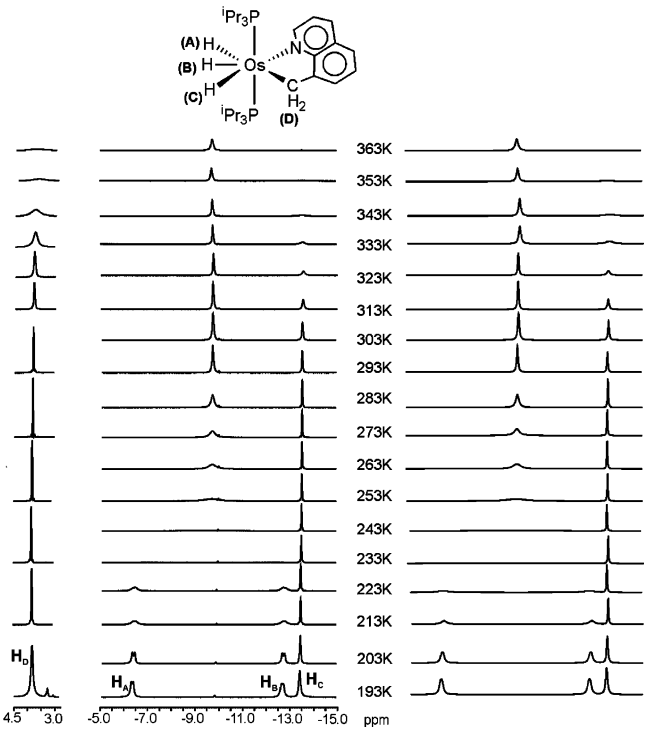

Figure 2. Variable-temperature ^{1}H{^{31}P} NMR spectra (300 MHz, toluene-d_8) of (**2**): experimental, methylene region (left); experimental, hydride region (center); calculated, hydride region (right).

In contrast to the ^{13}C{^{1}H} and ^{31}P{^{1}H} NMR spectra, the ^{1}H NMR spectrum is temperature dependent. Figure 2 collects the methylene and hydride resonances of the ^{1}H{^{31}P} NMR spectra between 363 and 193 K. The behavior of the signals is consistent with the operation of three thermally activated exchange processes, which have different activation parameters. That with the lowest energy barrier involves the hydride ligands **A** and **B**. Line-shape analysis of their signals between 203 and 283 K allows the calculation of the rate constants for the position exchange at these temperatures. The activation parameters obtained from the Eyring analysis are $\Delta H^{\ddagger} = 10.1 \pm 0.3$ kcal·mol^{-1} and $\Delta S^{\ddagger} = 1.6 \pm 0.8$ eu. The value for the activation entropy, close to zero, is in agreement with an intramolecular process, whereas the value for the activation enthalpy lies in the range reported for thermal exchange processes in related dihydride− and trihydride−osmium complexes (7−18 kcal·mol^{-1}).[12h,i,13a,b,14a−c,15b,16,18,19] The following position exchange in energy involves the hydride **C** and the hydrogen atoms of the methylene group of the heterometalacycle. Spin saturation transfer experiments between 268 and 298 K afford rate constants that lead to the activation parameters $\Delta H^{\ddagger} = 18.9 \pm 0.1$ kcal·mol^{-1} and $\Delta S^{\ddagger} = 3 \pm 2$ eu. The value of the activation enthalpy is significantly higher than that reported for the hydrogen exchange between the hydride and the methyl group of the complex $[OsH(\eta^5\text{-}C_5Me_5)(CH_3)(dmpm)]^+$ (7.1 ± 0.9 kcal·mol^{-1}; dmpm = bis(dimethylphosphino)methane).[7c] The third position exchange in energy takes place between the hydrides **C** and **B**. According to the spectra of Figure 2, the activation enthalpy in this case is certainly higher than that for the exchange between the hydride **C** and the methylene hydrogen atoms.

In methanol at −35 °C, crystals suitable for an X-ray diffraction study are formed. The data are consistent with the structure shown in eq 1. However, unfortunately, inaccurate structural parameters are obtained due to that the crystals undergo twinning (monoclinic space group *Cc* simulating *C*2/

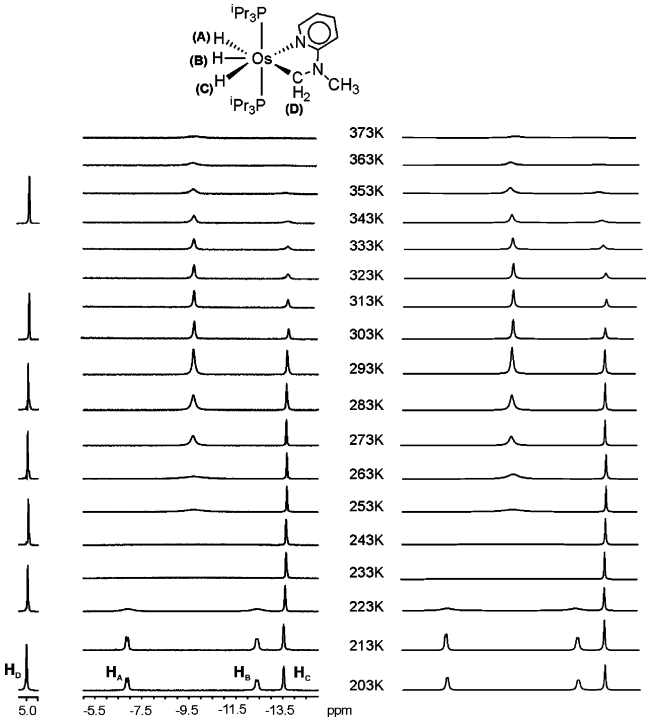

Figure 3. Variable-temperature $^1H\{^{31}P\}$ NMR spectra (300 MHz, toluene-d_8) of $OsH_3\{CH_2N(CH_3)$-*o*-$C_5H_4N\}(P^iPr_3)_2$ (**3**): experimental, methylene region (left); experimental, hydride region (center); calculated, hydride region (right).

c). DFT calculations provide useful accurate data for the hydrogen positions in both polyhydride and dihydrogen complexes.[12a,d,g,h,18,20] Thus, to determine the position of the hydrogen atoms bonded to the metal center, the structure of the model compound $OsH_3(CH_2C_9H_6N)(PMe_3)_2$ (**2t** in Figure 4, *vide infra*) has been optimized. The coordination around the osmium atom can be described as a distorted pentagonal bipyramid with the phosphorus atoms occupying axial positions (P−Os−P = 170.9°). The osmium sphere is completed by the metalated quinoline group, acting with a bite angle of 78.0°, and the hydride ligands. The Os−H bond lengths lie between 1.627 and 1.668 Å, whereas the H−H separations of 1.731 and 1.699 Å support the trihydride formulation.

The three hydrogen exchanges have also been theoretically studied. The associated transition states have been located and the energy barriers determined. The transition states for the hydride exchanges H_A-H_B and H_B-H_C have a dihydrogen nature. The exchange mechanism implies Os−H stretching, H−H shortening, and subsequent rotation of the resulting dihydrogen ligand. This mechanism has already been reported in a number of polyhydride compounds exhibiting hydride ligand exchanges.[1h,13,18a,20a] The calculated $\Delta E^{\ddagger}$ for the process involving the hydrides **A** and **B** (13.0 kcal·mol^{-1}) is significantly lower than that for the H_B-H_C exchange (21.2 kcal·mol^{-1}).

Scheme 1

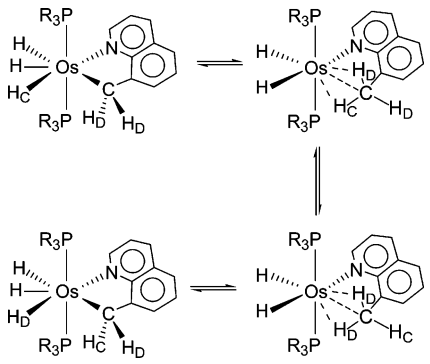

The exchange between the hydride **C** and the hydrogen atom of the methylene group (H_D) initially involves reductive coupling between H_C and the methylene substituent of the quinoline to afford a $-C(H_D)_2H_C$ methyl group. Subsequently, this substituent changes the orientation of the hydrogen atoms to allow the oxidative addition of a $C-H_D$ bond (Scheme 1). In agreement with the experimental observations, the calculated $\Delta E^{\ddagger}$ for the position exchange between the hydride **C** and the methylene hydrogen atoms (16.7 kcal·mol^{-1}) lies between those for the H_A-H_B and H_B-H_C exchanges.

Complex **1** also activates a $C(sp^3)-H$ bond of one of the methyl groups of the substituent of 2-(dimethylamino)pyridine. Treatment under reflux of toluene solutions of the hexahydride with 2.0 equiv of the organic substrate affords after 3 h the trihydride derivative $OsH_3\{CH_2N(CH_3)$-*o*-$C_5H_4N\}(P^iPr_3)_2$ (**3**), which is isolated as a yellow solid in 52% yield, according to eq 2. We note that, in contrast to **1**, the dihydride−iridium cation $[IrH_2(\kappa^1$-$OCMe_2)_2(PPh_3)_2]^+$ reacts with 2-(dimethylamino)-pyridine at room temperature to give the carbene compound $[IrH_2\{=CHN(CH_3)$-*o*-$C_5H_4N\}(PPh_3)_2]^+$. The reaction proceeds through the agostic and alkyl intermediates $[IrH_2\{CH_3N(CH_3)$-*o*-$C_5H_4N\}(PPh_3)_2]^+$ and $[IrH_2\{CH_2N(CH_3)$-*o*-$C_5H_4N\}(\eta^2$-$H_2)$-$(PPh_3)_2]^+$.[21]

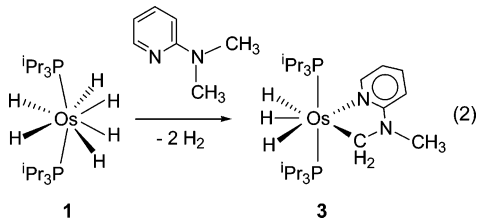

The spectroscopic data of **3** agree well with those of **2** and support the structure proposed in eq 2. In the $^{13}C\{^1H\}$ NMR spectrum, the $Os-CH_2$ resonance appears at 34.2 ppm, as a triplet with a C−P coupling constant of 6.2 Hz, whereas that corresponding to the NCH_3 methyl group is observed at 41.4

(18) See for example: (a) Castillo, A.; Barea, G.; Esteruelas, M. A.; Lahoz, F. J.; Lledós, A.; Maseras, F.; Modrego, J.; Oñate, E.; Oro, L. A.; Ruiz, N.; Sola, E. *Inorg. Chem.* **1999**, *38*, 1814. (b) Castarlenas, R.; Esteruelas, M. A.; Gutiérrez-Puebla, E.; Jean, Y.; Lledós, A.; Martín, M.; Tomàs, J. *Organometallics* **1999**, *18*, 4296.

(19) (a) Esteruelas, M. A.; Lahoz, F. J.; López, A. M.; Oñate, E.; Oro, L. A.; Ruiz, N.; Sola, E.; Tolosa, J. I. *Inorg. Chem.* **1996**, *35*, 7811. (b) Castillo, A.; Esteruelas, M. A.; Oñate, E.; Ruiz, N. *J. Am. Chem. Soc.* **1997**, *119*, 9691. (c) Baya, M.; Crochet, P.; Esteruelas, M. A.; Gutiérrez-Puebla, E.; Ruiz, N. *Organometallics* **1999**, *18*, 5034.

(20) (a) Barea, G.; Esteruelas, M. A.; Lledós, A.; López, A. M.; Tolosa, J. I. *Inorg. Chem.* **1998**, *37*, 5033. (b) Esteruelas, M. A.; Oro, L. A. *Adv. Organomet. Chem.* **2001**, *47*, 1. (c) Poli, R.; Baya, M.; Meunier-Prest, R.; Raveau, S. *New J. Chem.* **2006**, *30*, 759. (d) Belkova, N. V.; Revin, P. O.; Besora, M.; Baya, M.; Epstein, L. M.; Lledós, A.; Poli, R.; Shubina, E. S.; Vorontsov, E. V. *Eur. J. Inorg. Chem.* **2006**, 2192. (e) Baya, M.; Maresca, O.; Poli, R.; Coppel, Y.; Maseras, F.; Lledós, A.; Belkova, N. V.; Dub, P. A.; Epstein, L. M.; Shubina, E. S. *Inorg. Chem.* **2006**, *45*, 10248. (f) Tussupbayev, S.; Vyboishchikov, S. F. *Organometallics* **2007**, *26*, 56.

(21) (a) Lee, D.-H.; Chen, J.; Faller, J. W.; Crabtree, R. H. *Chem. Commun.* **2001**, 213. (b) Clot, E.; Chen, J.; Lee, D.-H.; Sung, S. Y.; Appelhans, L. N.; Faller, J. W.; Crabtree, R. H.; Eisenstein, O. *J. Am. Chem. Soc.* **2004**, *126*, 8795.

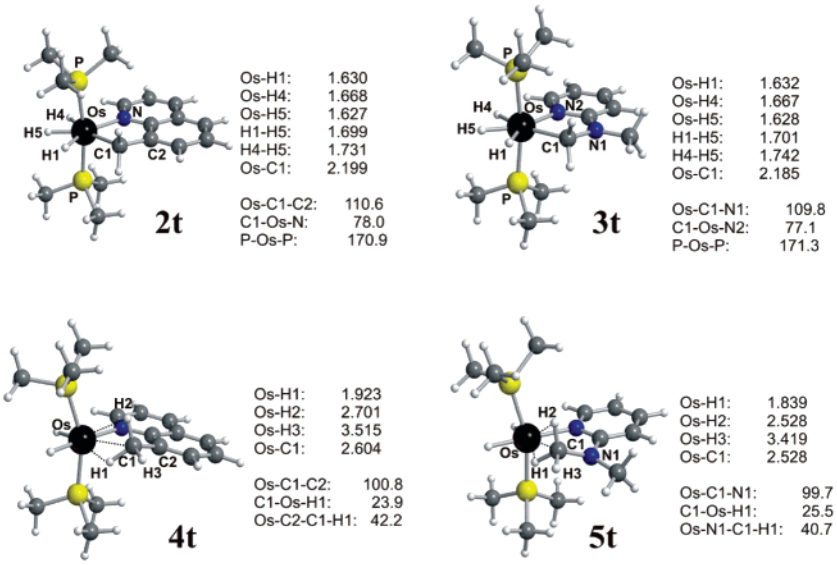

Figure 4. Optimized geometries of **2t** and **3t** (models of the experimental complexes **2** and **3**) and of the intermediates **4t** and **5t**, including a selection of distances (Å) and angles (deg).

ppm as a singlet. The $^{31}P\{^1H\}$ contains a singlet at 22.2 ppm, which is temperature invariant between 203 and 343 K. In this range of temperatures, the low-field region of the ^1H NMR spectrum is also temperature invariant. The most noticeable resonance of this part is that due to the methylene protons, which appears at 4.88 ppm as a triplet with a H−P coupling constant of 9.0 Hz. In contrast to the latter, the hydride resonances are temperature dependent (Figure 3). Between 373 and 253 K, the spectrum contains two signals at −9.68 and −13.53 ppm. At 223 K, the decoalescence of the signal at lower field occurs. Thus, at 203 K, three hydride resonances at −6.36, −12.75, and −13.47 ppm are clearly observed. They are assigned to the hydride ligands **A**, **B**, and **C**, respectively, on the basis of the NOESY spectrum at 203 K. Line-shape analysis of the hydride region allows the calculation of the rate constants for the thermal exchange processes at different temperatures. The activation parameters obtained from the corresponding Eyring analysis are $\Delta H^{\ddagger} = 9.6 \pm 0.3$ kcal·mol^{-1} and $\Delta S^{\ddagger} = 1.2 \pm 0.8$ eu for the H_A-H_B exchange and $\Delta H^{\ddagger} = 14.8 \pm 0.5$ kcal·mol^{-1} and $\Delta S^{\ddagger} = -4.7 \pm 1.3$ eu for the H_B-H_C exchange.

The comparison of the spectra of Figures 2 and 3 indicates that (i) the energy barrier for the position exchange between the hydride ligand disposed *cisoid* to the nitrogen atom (**A**) and the central one (**B**) is similar in both compounds, (ii) the energy barrier for the position exchange between the hydride ligand disposed *cisoid* to the methylene group (**C**) and **B** is higher for the quinoline derivative **2** than for the pyridine complex **3**, and (iii) the reductive elimination of CH_3 in **2** has an activation energy lower than in **3**.

Crystallization of **3** in methanol at −30 °C also affords crystals suitable for an X-ray diffraction study. In this case, they undergo a twinning by pseudomerohedry (monoclinic space group with $\beta \approx 90°$ that simulates orthorhombic), and, like for **2**, the obtained structural parameters are inaccurate. So, in order to confirm the trihydride nature of the complex, the structure of the model compound $OsH_3\{CH_2N(CH_3)$-*o*-$C_5H_4N\}(PMe_3)_2$ (**3t** in Figure 4, *vide infra*) was optimized by DFT calculations. The coordination around the osmium atom is like that of **2t**, i.e., a distorted pentagonal bipyramid with axial phosphines (P−Os−P = 171.3°). The Os−H bond lengths lie between 1.628 and 1.667 Å, whereas the H−H separations are 1.742 and 1.701 Å. The computed energy barriers for the hydride exchanges, 12.9 and 19.3 kcal·mol^{-1} for H_A-H_B and H_B-H_C, respectively, are considerably lower than the $\Delta E^{\ddagger}$ for exchange between the hydride **C** and the hydrogen atoms of the methylene group (24.7 kcal·mol^{-1}).

2. DFT Study of the Formation of 2 and 3 from 1: First C(sp^3)−H Bond Activation Process. The initial behavior of 8-methylquinoline and 2-(dimethylamino)pyridine toward the osmium hexahydride species is the same. Both react with **1**, affording the trihydride methylene complexes with release of two hydrogen molecules and C(sp^3)−H bond activation of the methyl substituent (eqs 1 and 2). The mechanism of the formation of **2** and **3** from **1** has been examined by DFT calculations. Views of the complete calculated energy profiles for these two reactions are shown in Figures 5 and 6.

This mechanism implies initial elimination of H_2 and coordination by a nitrogen atom of the pyridine-based ligand (**L$_1$** for **2** and **L$_2$** for **3**) to the resulting OsH_4 species (**1-H$_2$**), followed by a second dehydrogenation and subsequent C−H activation in a methyl group of the pyridinic ligand. Despite the mechanism of the processes affording **2** and **3** being the same, the theoretical study reveals subtle differences in the behavior of both pyridine ligands.

The energy cost for the H_2 elimination from the hexahydride in the $OsH_6(PMe_3)_2$ model complex is 29.3 kcal·mol^{-1}.[22] Coordination of the pyridinic ligands to the resulting unsaturated species, giving the intermediates (**1t-H$_2$)L$_1$** and (**1t-H$_2$)L$_2$**, produces stabilizations of about 10 and 13 kcal·mol^{-1}, respectively. The formation of these intermediates presents overall reaction energies of 19.9 and 16.1 kcal·mol^{-1}, respectively, with regard to the reactants. Although this process is strongly endothermic, it is thermodynamically driven by the irreversible loss of a dihydrogen molecule that is released away from the reaction media. Indeed, when considering entropic effects, the barrier for the H_2 elimination is considerably reduced (ΔG_{298} = 16.2 kcal·mol^{-1}). We note that both reactions proceed only in reflux toluene solutions (110 °C).

The following step, including a second hydrogen loss and H−C activation, is found to be thermodynamically favored in both cases. The final products **2t** and **3t** are 2.8 and 4 kcal·mol^{-1} more stable relative to (**1t-H$_2$)L$_1$** and (**1t-H$_2$)L$_2$**. Dehydroge-

(22) A lower value (15.8 kcal·mol^{-1}) was obtained for $OsH_6(PH_3)_2$ using the B3LYP functional.[12a]

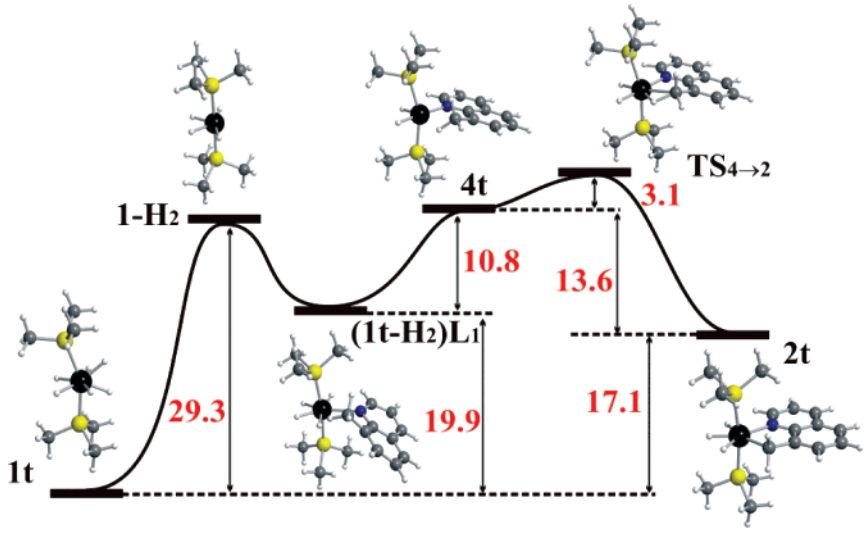

Figure 5. Calculated energy profile for the formation of **2t**, starting from **1t**.

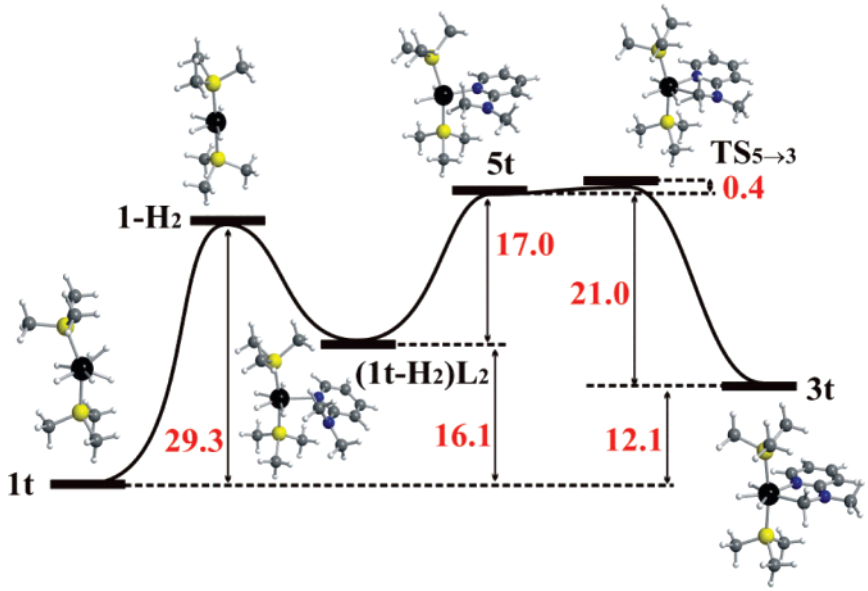

Figure 6. Calculated energy profile for the formation of **3t**, starting from **1t**.

nations of these latter intermediates are endothermic processes without transition states, leading to the unsaturated dihydrides **4t** and **5t**, respectively (Figure 4).

Intermediate $OsH_2(CH_3C_9H_6N)(PMe_3)_2$ (**4t**) can be described as an octahedral dihydride species, which is stabilized by η^3-H_2C coordination of the methyl substituent of the quinoline ligand (Figure 4). As expected for this coordination mode,[5] three very different separations between the metal center and the hydrogen atoms of the methyl group are observed, 1.923 Å (Os−H1), 2.701 Å (Os−H2), and 3.515 Å (Os−H3), whereas the Os−C1 distance is 2.604 Å. In agreement with the structural features experimentally found in δ-agostic complexes,[10] the angles Os−C1−C2 and C1−Os−H1 are 100.8° and 23.9°, respectively, and the dihedral angle between the planes Os, C2, C1 and C2, C1, H1 (Os−C2−C1−H1) has a value of 42.2°.

The model intermediate $OsH_2\{CH_3N(CH_3)$-o-$C_5H_4N\}(PMe_3)_2$ (**5t**) is similar to **4t** (Figure 4), with separations between the metal center and the atoms H1, H2, H3, and C1 of 1.839, 2.528, 3.419, and 2.528 Å, respectively. The angles Os−C1−N1 (99.7°) and C1−Os−H1 (25.5°) as well as the dihedral angle Os−N1−C1−H1 (40.7°) also agree well with the corresponding parameters of **4t**. Thus, in the pyridine intermediate **5t** the interaction of the methyl group with the osmium atom is stronger than that in the quinoline derivative **4t**. Note that in **5t** the separation between the metal center and the atoms of the methyl group are between 0.076 and 0.173 Å shorter than those in **4t**.

4t and **5t** are 10.8 and 17.0 kcal·mol^{-1} higher in energy than their precursors, respectively. However, the formation of **4t** and **5t** will be thermodynamically favored by the release of dihydrogen. The subsequent C−H activations require only 3.1 and 0.4 kcal·mol^{-1}, respectively (transition states: $\mathbf{TS_{4\to2}}$ and $\mathbf{TS_{5\to3}}$), thus rendering **2t** and **3t**, which are 13.6 and 21.0 kcal·mol^{-1} lower in energy than **4t** and **5t**. Transition state $\mathbf{TS_{4\to2}}$ can be regarded as a η^2-HC δ agostic derivative, which is the result of the approach of the atoms H1 (0.245 Å), H3 (0.346 Å), and C1 (0.247 Å) to the metal center and the estrangement of the hydrogen atom H2 (0.117 Å). The distortion is also evident in the C1−Os−H1 angle, which is opened up to 35.1°. On the other hand, the value of the dihedral angle Os−C2−C1−H1 diminishes to 33.8°. The transition state $\mathbf{TS_{5\to3}}$ connecting **5t** and **3t** is only 0.4 kcal·mol^{-1} above **5t** and has a geometry like that of $\mathbf{TS_{4\to2}}$. Like the latter, it is the result of the approach of the atoms H1 (0.128 Å), H3 (0.214 Å), and C1 (0.161 Å) to the metal and of the estrangement of H2 (0.272

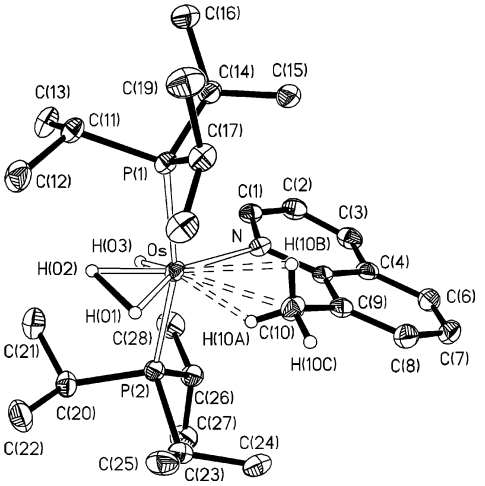

Figure 7. Molecular structure of the cation of **6** (ellipsoids are drawn at 50% probability). Selected bond lengths (Å) and angles (deg): Os−P(1) 2.3711(10), Os−P(2) 2.3562(10), Os−N 2.175(3), Os···C(10) 2.673(4), Os···H(10A) 2.01(4), Os···H(10B), 2.75(4), H(01)−H(02) 1.39(4), H(02)−H(03) 1.89(4); P(1)−Os−P(2) 165.63(3), P(1)−Os−N 98.12(8), P(2)−Os−N 93.64(8).

Å). However, the distortion with regard to **5t** is smaller than that observed for the activation of 8-methylquinoline. Thus, the C1−Os−H1 angle (32.3°) is opened up 8°, and the dihedral angle Os−N1−C1−H1 (40.1°) does not change significantly with regard to that of **5t**.

The calculated overall thermodynamic changes for the complete reactions leading from **1** to **2** and **3** are 17.1 and 12.1 kcal·mol^{-1}, respectively. The stabilizing power of the 2-aminopyridine assistant is revealed not only by the agostic intermediates but also by the trihydride−alkyl compounds. The 2-aminopyridine group stabilizes the trihydride−alkyl species better than the quinoline, as is deduced from the differences in energy between **4t** and **2t** and between **5t** and **3t**. Furthermore, the latter imposes an activation energy for the C(sp^3)−H bond activation process higher than the 2-aminopyridine assistant.

3. Protonation of 2 and 3: Coordination of the Methyl Group of 8-Methylquinoline and Second C(sp^3)−H Bond Activation on 2-(Dimethylamino)pyridine. Treatment at room temperature of diethyl ether solutions of **2** with 1.0 equiv of HBF_4·OEt_2 affords the hydride-elongated dihydrogen cation $[OsH(\eta^2\text{-}H_2)(CH_3C_9H_6N)(P^iPr_3)_2]BF_4$ (**6**), containing the methyl substituent of the quinoline ligand coordinated to the metal center in a η^3-H_2C fashion. This complex is isolated as a yellow solid in 77% yield, according to eq 3.

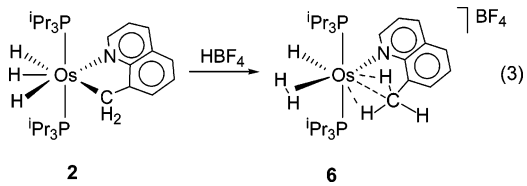

(3)

2 **6**

Complex **6** was characterized by elemental analysis, IR, $^{13}C\{^1H\}$, $^{31}P\{^1H\}$, and ^1H NMR spectroscopy, and an X-ray crystallographic study. Figure 7 shows an ORTEP drawing of the cation.

The coordination geometry around the osmium atom can be rationalized as being derived from a highly distorted octahedron with the two phosphine ligands occupying *trans* positions (P(1)−Os−P(2) = 165.63(3)°) at opposite sites of an ideal coordination plane defined by the three hydrogen atoms of the hydride and

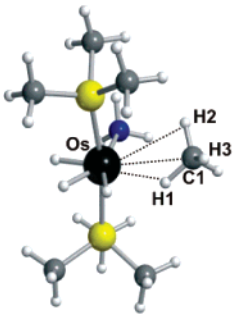

Os-H1: 2.046
Os-H2: 2.876
Os-H3: 3.415
Os-C1: 2.847

C1-Os-H1: 18.8

Figure 8. Optimized structure of the model complex $[OsH(\eta^2\text{-}H_2)(CH_4)(NH_3)(PMe_3)_2]^+$, including a selection of bond lengths (Å) and angles (deg).

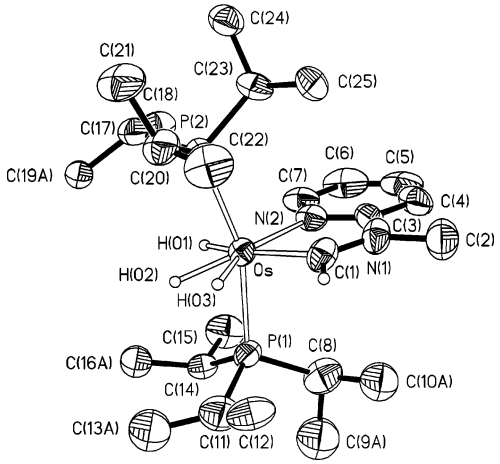

Figure 9. Molecular structure of the cation of **7** (ellipsoids are drawn at 50% probability). Selected bond lengths (Å) and angles (deg): Os−P(1) 2.3552(14), Os−P(2) 2.3548(15), Os−N(2) 2.144(5), Os−C(1) 1.988(6), N(1)−C(1) 1.349(7), N(1)−C(3) 1.369(7), N(2)−C(3) 1.341(7), H(01)−H(02) 1.82(7), H(02)−H(03) 1.45(7); P(1)−Os−P(2) 160.66(5), N(2)−Os−C(1) 73.9(2).

elongated dihydrogen ligands, mutually *cis* disposed, and the quinoline group. The η^3-H_2C coordination of the methyl substituent of the latter to the metal center is supported by the Os−H(10A), Os−H(10B), and Os−C(10) distances of 2.01(4), 2.75(3), and 2.673(4) Å, respectively. In agreement with **4t**, **5t**, and other experimentally characterized δ-agostic compounds,[10] the angles Os−C(10)−C(9) and Os−C(10)−H(10A) are 102.4(2)° and 14(1)°, whereas the dihedral angle between the planes Os, C(9), C(10) and C(9), C(10), H(10A) (Os−C(9)−C(10)−H(10A)) has a value of 34(3)°. The hydride-elongated dihydrogen character of the complex is consistent with the H(01)−H(02) and H(02)−H(03) separations of 1.39(4) and 1.89(4) Å, respectively. These structural parameters agree well with those obtained by DFT calculations on the optimized structure of the model compound $[OsH(\eta^2\text{-}H_2)(CH_3C_9H_6N)(PMe_3)_2]^+$ (**6t** in Figure 10, *vide infra*).

In order to further analyze the coordination mode of the methyl substituents in **6**, we have optimized the model complex $[OsH(\eta^2\text{-}H_2)(CH_4)(NH_3)(PMe_3)_2]^+$. The coordination of the methyl group of 8-methylquinoline to the osmium atom of the $[OsH(\eta^2\text{-}H_2)(P^iPr_3)_2]^+$ fragment, observed by X-ray diffraction, is similar to the coordination of methane to the metal center of the model fragment $[OsH(\eta^2\text{-}H_2)(NH_3)(PMe_3)_2]^+$ (Figure 8). In agreement with the experimental results, the Os−H1, Os−H2, and Os−C1 distances in the model complex $[OsH(\eta^2\text{-}H_2)(CH_4)(NH_3)(PMe_3)_2]^+$ are 2.046, 2.876, and 2.847 Å, respectively. This is an additional evidence showing that alkyl coordination

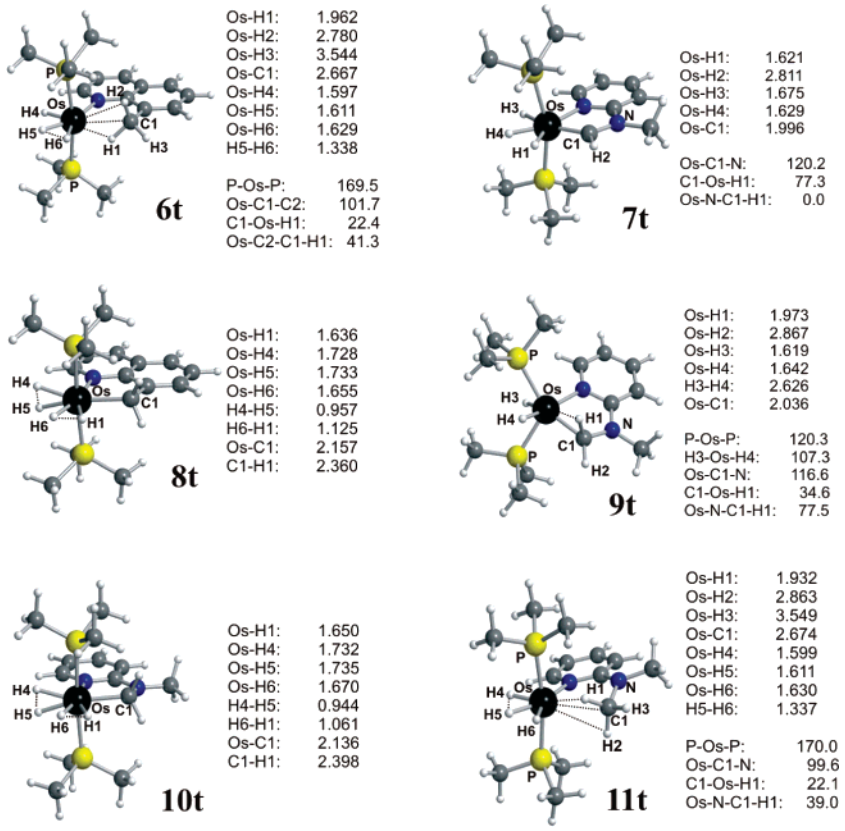

Figure 10. Optimized geometries of **6t** and **7t** (models of the experimental complexes **6** and **7**) and of the intermediates **8t, 9t**, **10t**, and **11t**, including a selection of distances (Å) and angles (deg).

in δ-agostic complexes is a satisfactory model to study the behavior of an alkane fixed at the coordination sphere of a transition metal.

The interaction between the methyl group and the osmium atom in **6** is also supported by the IR spectrum. Although the stretching frequencies of agostic bonds are difficult to observe, the IR of **6** in KBr clearly shows two weak ν(C−H) bands at 2732 and 2716 cm^{-1}, which are lower than the normal C−H stretches.[23] In contrast to the IR, the $^{13}C\{^1H\}$ NMR spectrum in dichloromethane-d_2 at room temperature does not show any signal for the methyl substituent of the quinoline ligand. However at 213 K, this group displays a singlet at −10.0 ppm, which is converted into a quartet with a C−H coupling constant of 121 Hz in the INEPT ^{13}C spectrum. This value is lower than that found for the methyl group of free 8-methylquinoline (128 Hz) and is an additional evidence of the agostic interaction. As expected for the *trans* disposition of the phosphine ligands, the $^{31}P\{^1H\}$ NMR spectra between 273 and 183 K contain a singlet at about 24 ppm.

In solution the hydrogen atoms of the methyl substituent of the quinoline and those of the elongated dihydrogen and hydride ligands exchange their positions. This is strongly supported by the ^1H NMR spectrum, which is also a function of the temperature. Between 293 and 253 K, the spectra do not show resonances due to the hydrogen atoms involved in the exchanges. Between 243 and 223 K, three broad signals are observed. At temperatures lower than 213 K, the exchanges are stopped and the spectra contain a singlet at 2.08 ppm, a broad resonance at −11.84 ppm, and a triplet with a H−P coupling constant of 13.7 Hz at −17.37 ppm, for the methyl substituent, the elongated dihydrogen, and hydride ligand, respectively. A variable-temperature 300 MHz T_1 study between 253 and 188 K of the elongated dihydrogen and hydride resonances gives $T_{1(min)}$ values of 31 ± 1 ms for the dihydrogen resonance and 91 ± 1 ms for the hydride signal, at 203 K. These values are consistent with the hydride-elongated dihydrogen character of the complex. In particular, the $T_{1(min)}$ value of the dihydrogen resonance corresponds to a hydrogen−hydrogen distance of 1.27 Å (slow spinning),[1c,24] which agrees well with that obtained by X-ray diffraction analysis.

There is a marked difference in reactivity between **2** and **3** toward $HBF_4{\cdot}OEt_2$. In contrast to **2**, the addition at room temperature of 1.0 equiv of this acid to diethyl ether solutions of **3** gives the cyclic carbene derivative [$OsH_3\{{=}CHN(CH_3)$-*o*-$C_5H_4N\}(P^iPr_3)_2$]BF_4 (**7**), as a result of the release of a hydrogen molecule and a C(sp^3)−H bond activation reaction on the methylene group of the heterometallacycle of **3**, i.e., as a result of a second C(sp^3)−H bond activation on one of the methyl groups of the substituent of 2-(dimethylamino)pyridine. Multiple C(sp^3)−H bond activation has been observed for methyl, dimethylamino, and methylene groups contained in phosphine ligands;[25] heterocyclic organic molecules such tet-

(23) (a) Brookhart, M.; Green, M. L. H. *J. Organomet. Chem.* **1983**, *250*, 395. (b) Brookhart, M.; Green, M. L. H.; Wong, L.-L. *Prog. Inorg. Chem.* **1988**, *36*, 1.

(24) (a) Earl, K. A.; Jia, G.; Maltby, P. A.; Morris, R. H. *J. Am. Chem. Soc.* **1991**, *113*, 3027. (b) Desrosiers, P. J.; Cai, L.; Lin, Z.; Richards, R.; Halpern, J. *J. Am. Chem. Soc.* **1991**, *113*, 4173.

(25) (a) Werner, H.; Weber, B.; Nürnberg, O.; Wolf, J. *Angew. Chem., Int. Ed. Engl.* **1992**, *31*, 1025. (b) Ingleson, M. J.; Yang, X.; Pink, M.; Caulton, K. G. *J. Am. Chem. Soc.* **2005**, *127*, 10846. (c) Rankin, M. A.; McDonald, R.; Ferguson, M. J.; Stradiotto, M. *Organometallics* **2005**, *24*, 4981. (d) Rankin, M. A.; McDonald, R.; Ferguson, M. J.; Stradiotto, M. *Angew. Chem., Int. Ed.* **2005**, *44*, 3603. (e) Carrión, M. C.; García-Vaquero, E.; Jalón, F. A.; Manzano, B. R.; Weissensteiner, W.; Mereiter, K. *Organometallics* **2006**, *25*, 4498. (f) Weng, W.; Parkin, S.; Ozerov, O. V. *Organometallics* **2006**, *25*, 5345.

rahydrofuran, pyrrolidine, and dioxolane;[26] linear ethers;[27] cresols;[28] carbonyl compounds;[16,29] and hydrocarbons.[30] Complex **7** is isolated as an orange solid in 94% yield, according to eq 4.

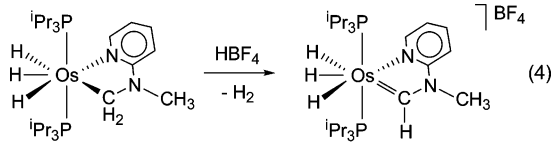

3 **7**

Like **6**, complex **7** was characterized by elemental analysis, MS, IR, $^{13}C\{^1H\}$, $^{31}P\{^1H\}$, and ^1H NMR spectroscopy, and an X-ray crystallographic study. Figure 9 shows an ORTEP drawing of the cation.

The coordination geometry around the osmium atom can be described as a distorted pentagonal bipyramid with the phosphine ligands occupying axial positions (P(1)−Os−P(2) = 160.66(5)°). The metal sphere is completed by the doubly activated 2-(dimethylamino)pyridine ligand, acting with a bite angle of 73.9(2)°, and the hydride ligands. The Os−C(1) bond length of 1.988(6) Å supports the Os−C double bond formulation.[17b,31] In agreement with the sp^2 hybridization at C(1), the angles around this atom are about 120°. The separations between the hydrogen atoms bonded to the metal center are 1.82(7) Å (H(01)−H(02)) and 1.45(7) Å (H(02)−H(03)). These structural parameters agree well with those obtained by DFT calculations on the optimized structure of the model compound $[OsH_3\{=CHN(CH_3)\text{-}o\text{-}C_5H_4N\}(PMe_3)_2]BF_4$ (**7t** in Figure 10, *vide infra*).

In agreement with the mutually *trans* disposition of the phosphine ligands, the $^{31}P\{^1H\}$ NMR spectrum contains a singlet at 36.3 ppm. The presence of the doubly activated 2-(dimethylamino)pyridine ligand is also evident in the $^{13}C\{^1H\}$ NMR spectrum, which shows a singlet at 248.1 ppm corresponding to the OsC-carbon atom of the heterometallacycle. In the ^1H NMR spectrum at room temperature, the OsCH resonance appears at 12.80 ppm as a quartet with a H−H coupling constant of 5.0 Hz, by spin coupling with the hydride ligands. The latter displays at −8.36 ppm a double triplet with a H−P coupling constant of 14.7 Hz. This observation is consistent with the operation of two thermally activated site exchange processes for the hydride ligands, which proceed at rates sufficient to lead to the single resonance. Consistent with this, lowering the sample temperature produces a broadening of the resonance. Between 223 and 203 K decoalescence occurs. Because the activation energy of both exchange processes is similar, decoalescence directly gives the ABC part of an $ABCMX_2$ spin system with $\delta_A = -5.0$, $\delta_B = -9.5$, $\delta_C = -11.5$, $J_{AB} = 317$ Hz, $J_{AC} = 10$ Hz, and $J_{BC} = 400$ Hz, which is clearly observed at 183 K. The large values of J_{AB} and J_{BC} suggest the operation of quantum exchange coupling[31] between H_A and H_B, and H_B and H_C.

4. DFT Study of the Evolution of 2 and 3 after Protonation. The protonation of the neutral trihydride−methylene compounds **2** and **3** proceeds in a different way. The reaction of **2** with HBF_4 affords a hydride−dihydrogen cation containing an agostic methyl substituent (**6**), whereas protonation of **3** leads to a trihydride carbene species **7** (eqs 3 and 4). These reactions have been modeled and studied by DFT calculations.

Several isomers are conceivable as products of the protonation of **2**. The formation of the experimentally detected **6** could take place by direct protonation of the methylene group of the heterometallacycle of **2** or by addition of the proton of the acid to the OsH_3 unit and the subsequent hydrogen migration from the osmium to the carbon atom of the methylene group. The different possibilities have been theoretically explored. The hydride−dihydrogen−methyl **6t**, discussed above, is found to be the most stable isomer. Two other minima, with an "OsH_4" unit resulting from the protonation of the OsH_3 unit of **2**, have also been located: the dihydrogen (H4−H5 = 0.957 Å)-elongated dihydrogen (H1−H6 = 1.125 Å) $[Os(\eta^2\text{-}H_2)_2(CH_2C_9H_6N)(PMe_3)_2]^+$ (**8t**) and a bis-dihydrogen isomer (H−H = 0.909 and 0.994 Å) (**8t′**) that is 3.6 kcal·mol^{-1} less stable than **8t**.

The dihydrogen ligand of **8t** (Figure 10) is parallel to the P−Os−P direction and lies *trans* to the carbon atom of the heterometallacycle (C1). The elongated dihydrogen ligand is contained in the plane perpendicular to the P−Os−P direction and is disposed *cis* to C1. Intermediate **8t** is 3.8 kcal·mol^{-1} less stable than **6t**. It is clear that the thermodynamically favored species is that originated by formal electrophilic attack on the carbon atom. These results are in good agreement with the experimental observation of **6**.

Starting from **8t** it is possible to obtain **6t** by C−H reductive elimination, in a process similar to that operating for the hydride-H methylene exchange in **2** (see above). The energy profile for the isomerization process is depicted in Figure 11. The transition state $\mathbf{TS_{8\to6}}$ connecting both species is located 13.3 kcal·mol^{-1} above **8t**. It results from the approach of H1 to C1 in **8t**. As a consequence of this, the osmium−hydride−methylene unit forms an η^2-HC δ-agostic derivative with coordination parameters for the methyl group very similar to those of $\mathbf{TS_{4\to2}}$.

The low activation energy calculated for the rupture of a $C(sp^3)$−H bond of the methyl substituent of the quinoline ligand to give **8t** (17.1 kcal·mol^{-1}) is consistent with the observed hydrogen exchange in solution between the metal center and the agostic methyl group of **6**. In addition, it should be mentioned that this barrier is similar to that calculated for the position exchange between the hydride and the hydrogen atoms of the elongated dihydrogen ligand in **6t** (15.4 kcal·mol^{-1}). This indicates that, once coordinated to the metal sphere, the rupture

(26) (a) Boutry, O.; Gutiérrez, E.; Monge, A.; Nicasio, M. C.; Pérez, P. J.; Carmona, E. *J. Am. Chem. Soc.* **1992**, *114*, 7288. (b) Gutiérrez-Puebla, E.; Monge, A.; Nicasio, M. C.; Pérez, P. J.; Poveda, M. L.; Carmona, E. *Chem.−Eur. J.* **1998**, *4*, 2225. (c) Slugovc, C.; Mereiter, K.; Trofimenko, S.; Carmona, E. *Angew. Chem., Int. Ed.* **2000**, *39*, 2158. (d) Ferrando-Miguel, G.; Coalter, J. N., III; Gérard, H.; Huffman, J. C.; Eisenstein, O.; Caulton, K. G. *New J. Chem.* **2002**, *26*, 687.

(27) (a) Santos, L. L.; Mereiter, K.; Paneque, M.; Slugovc, C.; Carmona, E. *New J. Chem.* **2003**, *27*, 107. (b) Carmona, E.; Paneque, M.; Santos, L. L.; Salazar, V. *Coord. Chem. Rev.* **2005**, *249*, 1729.

(28) Lara, P.; Paneque, M.; Poveda, M. L.; Salazar, V.; Santos, L. L.; Carmona, E. *J. Am. Chem. Soc.* **2006**, *128*, 3512.

(29) Grotjahn, D. B.; Hoerter, J. M.; Hubbard, J. L. *J. Am. Chem. Soc.* **2004**, *126*, 8866.

(30) Lee, J.-H.; Pink, M.; Caulton, K. G. *Organometallics* **2006**, *25*, 802.

(31) (a) Esteruelas, M. A.; Lahoz, F. J.; López, A. M.; Oñate, E.; Oro, L. A. *Organometallics* **1994**, *13*, 1669. (b) Esteruelas, M. A.; Lahoz, F. J.; Oñate, E.; Oro, L. A.; Valero, C.; Zeier, B. *J. Am. Chem. Soc.* **1995**, *117*, 7935. (c) Brumaghim, J. L.; Girolami, G. S. *Chem. Commun.* **1999**, 953. (d) Werner, H.; Stüer, W.; Wolf, J.; Laubender, M.; Weberndörfer, B.; Herbst-Irmer, R.; Lehmann, C. *Eur. J. Inorg. Chem.* **1999**, 1889. (e) Castarlenas, R.; Esteruelas, M. A.; Oñate, E. *Organometallics* **2001**, *20*, 2294. (f) Gusev, D. G.; Lough, A. J. *Organometallics* **2002**, *21*, 2601. (g) Weberndörfer, B.; Henig, G.; Hockless, D. C. R.; Bennett, M. A.; Werner, H. *Organometallics* **2003**, *22*, 744. (h) Castarlenas, R.; Esteruelas, M. A.; Oñate, E. *Organometallics* **2005**, *24*, 4343. (i) Bolaño, T.; Castarlenas, R.; Esteruelas, M. A.; Modrego, F. J.; Oñate, E. *J. Am. Chem. Soc.* **2005**, *127*, 11184. (j) Esteruelas, M. A.; Fernández-Alvarez, F. J.; Oliván, M.; Oñate, E. *J. Am. Chem. Soc.* **2006**, *128*, 4596.

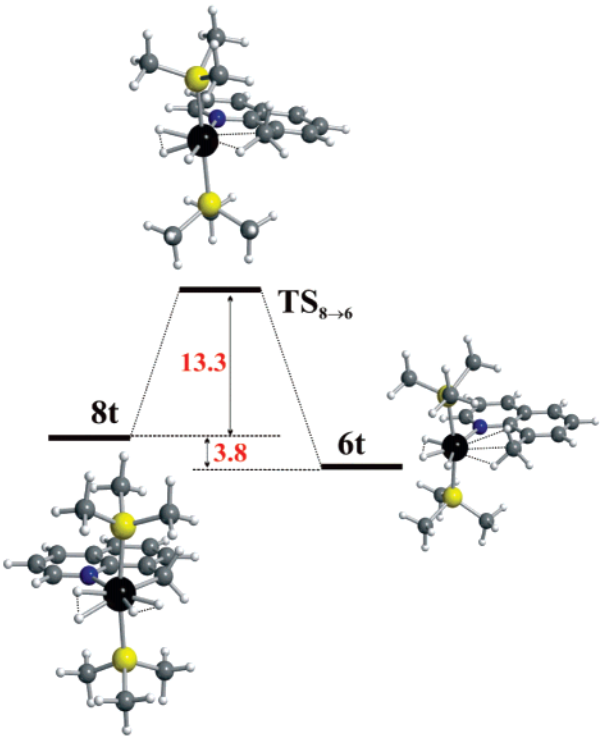

Figure 11. Calculated energy profile for the isomerization of [Os(η^2-H_2)$_2$($CH_2C_9H_6N$)(PMe_3)$_2$]$^+$ (**8t**) to [OsH(η^2-H_2)($CH_3C_9H_6N$)(PMe_3)$_2$]$^+$ (**6t**).

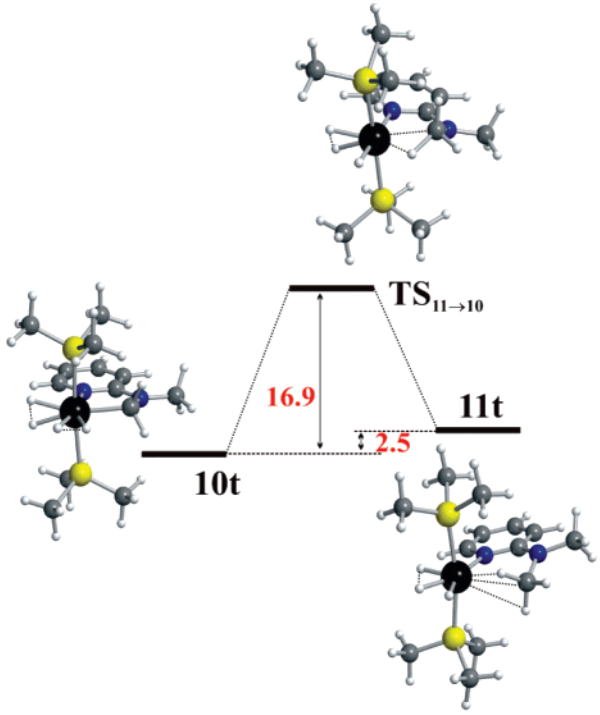

Figure 12. Calculated energy profile for the isomerization of [Os(η^2-H_2)$_2${$CH_2N(CH_3)$-*o*-C_5H_4N}(PMe_3)$_2$]$^+$ (**10t**) to [OsH(η^2-H_2)-{$CH_3N(CH_3)$-*o*-C_5H_4N}(PMe_3)$_2$]$^+$ (**11t**).

processes of the H−H and C(sp³)−H bonds have similar activation barriers.

As found in the theoretical study of the protonation of **2**, three minima have been obtained as products of the protonation of **3** (Figure 10). Two of them (**10t** and **10t′**) have bis(dihydrogen) character and arise from the protonation of the "OsH_3" unit of **3**, presenting structures very similar to those found in the protonation of the "OsH_3" unit of **2** (**8t** and **8t′**). The third one (**11t**) results from the protonation of the methylene group of the heterometallacycle, and it is equivalent to the product **6t** obtained in the protonation of **3**. Interestingly with the 2-(dimethylamino)pyridine ligand the resulting complex [OsH(η^2-H_2)-{$CH_3N(CH_3)$-*o*-C_5H_4N}(PMe_3)$_2$]$^+$ (**11t**) is less stable (2.5 kcal·mol^{-1}) than the dihydrogen (H4−H5 = 0.944 Å)-elongated dihydrogen (H1−H6 = 1.061 Å) [Os(η^2-H_2)$_2${$CH_2N(CH_3)$-*o*-C_5H_4N}(PMe_3)$_2$]$^+$ (**10t**, Figure 12).

In order to understand why the behavior of **3** is different from that of **2**, we have also analyzed the hydrogen migration from the metal center to the methylene carbon in **10t** (Figure 12). The resulting intermediate **11t**, which is the species equivalent to the product **6t** obtained with the 8-methylquinoline ligand, is found 2.5 kcal·mol^{-1} above **10t**. The transition state (**TS$_{11\rightarrow10}$**) for the C−H activation connecting **10t** and **11t** lies 16.9 kcal·mol^{-1} above **10t**.

The dissociation of a hydrogen molecule from dihydrogen-elongated dihydrogen intermediate **10t** affords an unsaturated OsH_2 species, which should evolve into **7** by an α-elimination reaction. The structures of the OsH_2 species resulting from the dihydrogen elimination in **10t** have also been optimized. Three minima have been found: a dihydrogen (H−H = 0.912 Å), an elongated dihydrogen (H−H = 1.251 Å), and a dihydride (H−H = 2.626 Å). The dihydrogen and elongated dihydrogen compounds are 27.5 and 14.1 kcal·mol^{-1}, respectively, less stable than the dihydride (**9t**). The calculated $\Delta G^{\ddagger}$ for the dissociation of a hydrogen molecule from **10t** to afford **9t** is 18.6 kcal·mol^{-1}.

Both dihydrogen compounds have octahedral structures, while the coordination geometry of the dihydride is similar to those found in the complexes $OsH_2Cl_2(P^iPr_3)_2$[33] and OsH_2{κ^2-O,S−OC(=O)[NHC(=O)CH_3]CH_2S}(P^iPr_3)$_2$[34] by X-ray diffraction analysis, with P−Os−P and H−Os−H angles of 120.3° and 107.3°, respectively. Another interesting feature of this [OsH_2-{$CH_2N(CH_3)$-*o*-C_5H_4N}(PMe_3)$_2$]$^+$ (**9t**) dihydride is the very short separation between the metal center and the H1 hydrogen atom of the methylene group of the heterometallacycle. Its value of 1.973 Å is consistent with an α-agostic interaction[35] and suggests than the C−H activation leading to the trihydride carbene species **7**, the experimentally observed product, is an easy process. Intermediate **9t** is 3.9 kcal·mol^{-1} less stable than the final product **7t** (Figure 13).

The transfer of H1 from C1 to the metal center takes place through the transition state **TS$_{9\rightarrow7}$**, which lies 9.7 kcal·mol^{-1} above **9t**. The eigenvector associated with its unique imaginary frequency is mainly related to the elongation of the activating H−C bond. This species can be described as a trihydride compound. Its structure is similar to those of complexes $OsH_2X(\kappa^2$-$O_2CCH_3)(P^iPr_3)_2$ (X = Cl, κ^1-$OC(O)CH_3$);[36] that is, if one takes as a base the structure of $OsH_2Cl_2(P^iPr_3)_2$ or **9t**,

(32) Sabo-Etienne, S.; Chaudret, B. *Chem. Rev.* **1998**, *98*, 2077.
(33) Aracama, M.; Esteruelas, M. A.; Lahoz, F. J.; López, J. A.; Meyer, U.; Oro, L. A.; Werner, H. *Inorg. Chem.* **1991**, *30*, 288.
(34) Atencio, R.; Esteruelas, M. A.; Lahoz, F. J.; Oro, L. A.; Ruiz, N. *Inorg. Chem.* **1995**, *34*, 1004.
(35) Goddard, R. J.; Hoffmann, R.; Jemmis, E. D. *J. Am. Chem. Soc.* **1980**, *102*, 7667.
(36) Crochet, P.; Esteruelas, M. A.; López, A. M.; Martínez, M. P.; Oliván, M.; Oñate, E.; Ruiz, N. *Organometallics* **1998**, *17*, 4500.

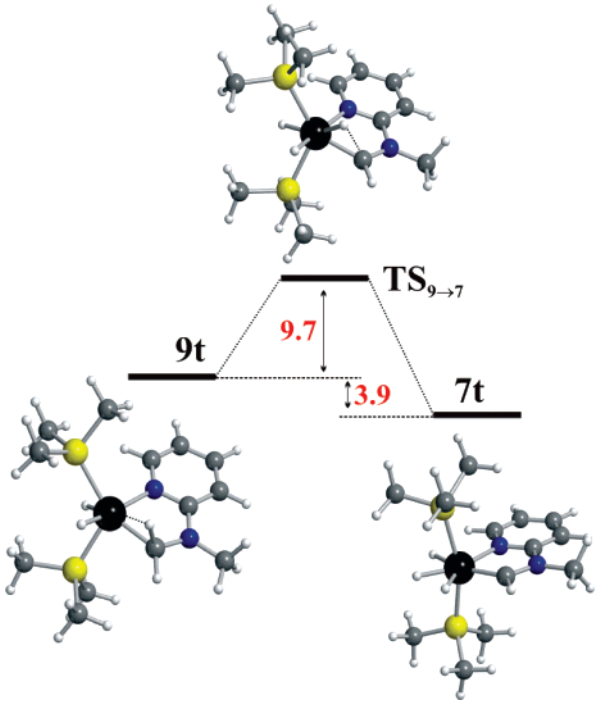

Figure 13. Calculated energy profile for the conversion of [OsH_2{$CH_2N(CH_3)$-*o*-C_5H_4N}$(PMe_3)_2$]$^+$ (**9t**) to [OsH_3{=$CHN(CH_3)$-*o*-C_5H_4N}$(PMe_3)_2$]$^+$ (**7t**).

the geometry around the metal center can be seen as derived from a distorted square antiprism with a missing vertex. One of two square planes is made up by the two phosphine atoms and the hydride ligands H3 and H4, which occupy alternate positions. The atoms C1, N, and the hydride ligand H1 are located in the second plane.

With the 2-(dimethylamino)pyridine ligand the activation barrier for the hydrogen migration from the metal center to the methylene carbon atom in the dihydrogen-elongated dihydrogen intermediate **10t** formed after protonation of **3** is higher (16.9 kcal·mol^{-1}) than for the 8-methylquinoline system (13.3 kcal·mol^{-1}, Figure 11). Furthermore, in contrast to **6t**, the resulting complex [$OsH(\eta^2$-$H_2)${$CH_3N(CH_3)$-*o*-C_5H_4N}$(PMe_3)_2$]$^+$ (**11t**) is less stable (2.5 kcal·mol^{-1}) than its precursor. The higher activation barrier and the lower stability of the resulting species from the hydrogen-transfer process can explain why contrary to what happens with **8t** → **6t** transformation, the dihydrogen-elongated dihydrogen intermediate (**10t**) prefers to release a hydrogen molecule and evolves into the trihydride−carbene complex instead of evolving into trihydride methyl (**11t**).

Concluding Remarks

This study has revealed that the coordination of 8-methylquinoline and 2-(dimethylamino)pyridine to osmium−hydride fragments of 14-valence electrons affords methyl δ-agostic species, where the structural parameters for the methyl coordination are similar to those for the coordination of methane. Therefore, complexes of this type are satisfactory models to study, in some aspect, the behavior of alkanes fixed at the coordination sphere of a transition metal.

The activation energy for the rupture of a coordinated C(sp^3)−H bond is similar to that for the rupture of a coordinated H−H bond. As a consequence, hydrogen exchange processes between hydride, dihydrogen, and a methyl group occur, in a competitive manner, in hydride and dihydrogen complexes stabilized by δ-agostic interaction between the metal center and a methyl group of coordinated 8-methylquinoline or 2-(dimethylamino)pyridine.

The activation energies for the position exchanges between hydride and dihydrogen ligands are not very sensitive to the coordination assistance of the methyl group, quinoline, or 2-aminopyridine. However, the hydrogen exchanges between hydride or dihydrogen ligands and the coordinated methyl group show a noticeable dependence, since the coordination assistant carries out the fine-tuning of the stabilities and activation energies involving the metal−methyl unit. With regard to the quinoline group, the 2-aminopyridine assistant provides lower activation energies for the C(sp^3)−H bond rupture and higher stabilities of the resulting alkyl derivatives. Furthermore, it facilitates a second C(sp^3)−H bond activation.

Experimental Section

General Procedures. All reactions were carried out under an argon atmosphere using Schlenk tube techniques. Solvents were dried and purified by known procedures and distilled under argon prior to use. The complex $OsH_6(P^iPr_3)_2$ (**1**) was prepared as previously described.[33]

Physical Measurements. C, H, and N analyses were measured on a Perkin-Elmer 2400 CHNS/O analyzer. Infrared spectra were recorded on a Perkin-Elmer Spectrum One spectrometer as solids (Nujol mull or KBr pellet). ^{1}H, ^{1}H NOESY, ^{13}C{^{1}H}, ^{13}C, and ^{31}P{^{1}H} NMR spectra were recorded on Varian Gemini 2000, Bruker AXR 300, and Bruker Avance 400 instruments. Chemical shifts are referenced to residual solvent peaks (^{1}H and ^{13}C{^{1}H}) and external H_3PO_4 (^{31}P{^{1}H}). Coupling constants J and N ($N = J_{P-H} + J_{P'-H}$ for ^{1}H; $N = J_{P-C} + J_{P'-C}$ for ^{13}C{^{1}H}) are given in hertz.

Kinetic Analyses. ^{1}H{^{31}P} Spectral Simulation. Experimental exchange broadened line shapes were iteratively fit using the gNMR[37] program, with the line width in the absence of exchange fixed at the lowest measured values. Spin saturation transfer measurements were performed according to the Forsén−Hoffman method[38] by irradiating the resonance assigned to H_c and measuring the integral of the resonance of the $-CH_2-$ group. The exchange rates were calculated from the equation $k = (1/T_1)((I/I') - 1)$, where I' and I are the integrals for the resonance of the $-CH_2-$ group with and without saturation of the resonance of H_c. T_1 is the spin−lattice relaxation time of the signal of the $-CH_2-$ group obtained by the inversion−recovery method in the presence of the saturating field at the hydride H_c signal.[39] In all cases, the activation parameters, $\Delta H^{\ddagger}$ and $\Delta S^{\ddagger}$, were obtained from a linear least-squares fit of ln(k/T) vs 1/T (Eyring equation). Errors were computed by published methods.[40] The error in temperature was assumed to be 1 K; error in k was estimated as 10%.

Preparation of $OsH_3(CH_2C_9H_6N)(P^iPr_3)_2$ (2). A colorless solution of **1** (200 mg, 0.386 mmol) in 15 mL of toluene was treated with 1.5 equiv of 8-methylquinoline (98.6 μL, 0.766 mmol) and heated under reflux for 1.5 h. The resulting solution was filtered through Celite and dried *in vacuo*. Methanol was added to afford a red solid, which was washed with further portions of methanol and dried *in vacuo*. Yield: 170 mg (97%). Anal. Calcd for $C_{28}H_{53}$-

(37) Budzelaar, P. H. M. *gNMR*, version 4.1; Ivory Soft: Englewood, CO, 1999 (Published by Cherwell Scientific Publishing Limited, Oxford, U.K.).

(38) (a) Faller, J. W. In *Determination of Organic Structures by Physical Methods*; Nachod, F. C., Zuckerman, J. J., Eds.; Academic Press: New York, 1973. (b) Sanders, J. K. M.; Hunter, B. K. *Modern NMR Spectroscopy, A Guide for Chemists*, 2nd ed.; Oxford University Press, 1993.

(39) Mann, B. E. *J. Magn. Reson.* **1977**, *25*, 91.

(40) Morse, P. M.; Spencer, M. D.; Wilson, S. R.; Girolami, G. S. *Organometallics* **1994**, *13*, 1646.

$NOsP_2$: C, 51.27; H, 8.15; N, 2.13. Found: C, 51.50; H, 7.90; N, 2.28. IR (Nujol, cm^{-1}): ν(OsH) 2017 (s), 2125 (s). ^1H NMR (300 MHz, C_6D_6, 293 K): δ 9.95 (d, $J_{H-H} = 8.1$, 1H, C_9H_6), 7.73 (d, $J_{H-H} = 7.3$, 1H, C_9H_6), 7.37 (d, $J_{H-H} = 8.1$, 1H, C_9H_6), 7.18 (t, $J_{H-H} = 7.3$, 1H, C_9H_6), 7.02 (d, $J_{H-H} = 7.3$, 1H, C_9H_6), 6.37 (dd, $J_{H-H} = 8.1$, 1H, C_9H_6), 3.78 (t, $J_{H-P} = 5$, 2H, $-CH_2$), 2.02 (m, 6H, PC*H*$(CH_3)_2$), 1.07 (dvt, $N = 12.3$, $J_{H-H} = 6$, 18H, PCH(C*H*$_3)_2$), 0.92 (dvt, $N = 12$, $J_{H-H} = 6$, 18H, PCH(C*H*$_3)_2$), −9.68 (br, 2H, OsH), −13.53 (t, $J_{H-P} = 13$, 1H, OsH). ^1H {^{31}P} NMR (300 MHz, C_7D_8, 203 K, methylene and hydride region): δ 3.78 (s, 2H, $-CH_2$), −6.36 (d, $J_{H-H} = 30$, 1H) −12.75 (d, $J_{H-H} = 30$, 1H), −13.47 (s, 1H). $^{31}P\{^1H\}$ NMR (121.42 MHz, C_6D_6, 293 K): δ 23.1 (s). $^{13}C\{^1H\}$ NMR (100.56 MHz, C_6D_6, 293 K, plus apt): δ 159.4 (s, C_9H_6), 156.7 (s, C_9H_6), 155.9 (s, C_9H_6), 133.9 (s, C_9H_6), 132.4 (s, C_9H_6), 129.8 (s, C_9H_6), 127.0 (s, C_9H_6), 122.2 (s, C_9H_6), 122.0 (s, C_9H_6), 27.0 (vt, $N = 21.9$, PC*H*$(CH_3)_2$), 20.2, 19.8, (both s, PCH(C*H*$_3)_2$), 6.7 (t, $J_{C-P} = 5$, $-CH_2-$). MS (FAB$^+$): *m*/*z* 655 ($M^+ - 1H$). $T_{1(min)}$ (ms, OsH, 300 MHz, C_7D_8, 228 K): 94.6 ± 3 (−6.42 ppm, −12.72 ppm), 116.4 ± 1 (−13.45 ppm).

Preparation of $OsH_3\{CH_2N(CH_3)$-*o*-$C_5H_4N\}(P^iPr_3)_2$ (3). A colorless solution of **1** (125 mg, 0.242 mmol) in 15 mL of toluene was treated with 2 equiv of 2-(dimethylamino)pyridine (59.2 μL, 0.484 mmol) and heated under reflux for 3 h. The resulting yellow solution was filtered through Celite and dried *in vacuo*. Methanol was added to afford a yellow solid, which was washed with further portions of methanol and dried *in vacuo*. Yield: 80 mg (52%). Anal. Calcd for $C_{25}H_{54}N_2OsP_2$: C, 47.29; H, 8.57; N, 4.41. Found: C, 47.30; H, 8.66; N, 4.21. IR (Nujol, cm^{-1}): ν(OsH) 2020 (s), 2109 (s). ^1H NMR (300 MHz, C_7D_8, 293 K): δ 8.96 (d, $J_{H-H} = 6.8$, 1H, py), 6.82 (t, $J_{H-H} = 6.8$, 1H, py), 5.77 (t, $J_{H-H} = 6.8$, 1H, py), 5.55 (d, $J_{H-H} = 6.8$, 1H, py), 4.88 (t, $J_{H-P} = 9$, 2H, $-CH_2-$), 2.77 (s, 3H, CH_3), 2.06 (m, 6H, PC*H*$(CH_3)_2$), 1.14 (dvt, $N = 12.6$, $J_{H-H} = 6.6$, 18H, PCH(C*H*$_3)_2$), 1.10 (dvt, $N = 12$, $J_{H-H} = 6.6$, 18H, PCH(C*H*$_3)_2$ −9.73 (br, 2H, OsH), −13.72 (br, 1H, OsH). $^1H\{^{31}P\}$ NMR (300 MHz, C_7D_8, 203 K, hydride region): δ −7.54 (d, $J_{H-H} = 23$, 1H), −13.07 (d, $J_{H-H} = 23$, 1H), −14.17 (s, 1H). $^{31}P\{^1H\}$ NMR (121.42 MHz, C_7D_8, 293 K): δ 22.2 (s). $^{13}C\{^1H\}$ NMR (75.42 MHz, C_6D_6, 293 K): δ 162.3 (s, C_{ipso}, py), 158.1 (s, py), 133.7 (s, py), 109.9 (s, py), 104.8 (s, py), 41.4 (s, CH_3), 34.2 (t, $J_{C-P} = 6.2$, $-CH_2-$), 26.7 (vt, $N = 22$, PC*H*$(CH_3)_2$), 20.3, 19.8, (both s, PCH(C*H*$_3)_2$). $T_{1(min)}$ (ms, OsH, 300 MHz, C_7D_8): 107.6 ± 1 (−13.53 ppm, 223 K), 96 ± 1 (−6.86 ppm, −12.40 ppm, 218 K). MS (FAB$^+$): *m*/*z* 631 ($M^+ - 2H$).

Preparation of $OsH(\eta^2\text{-}H_2)(CH_3C_9H_6N)(P^iPr_3)_2]BF_4$ (6). A red solution of **2** (210 mg, 0.320 mmol) in 30 mL of diethyl ether was treated with 1 equiv of $HBF_4{\cdot}OEt_2$ (45 μL, 0.320 mmol) and stirred for 30 min at room temperature. During the course of the reaction a yellow solid formed. The solvent was removed, and the solid was washed with further portions of diethyl ether and dried *in vacuo*. Yield: 182 mg (77%). Anal. Calcd for $C_{28}H_{54}BF_4NOsP_2$: C, 45.22; H, 7.32; N, 1.88. Found: C, 45.16; H, 7.21; N, 2.01. IR (KBr, cm^{-1}): ν(OsH) 2137 (s), 2183 (s); ν(Os−$H_{agostic}$) 2716 (w), 2732 (w). ^1H NMR (300 MHz, CD_2Cl_2, 213 K): δ 9.25 (d, $J_{H-H} = 4.9$, 1H, C_9H_6), 8.29 (d, $J_{H-H} = 7.6$, 1H, C_9H_6), 7.78 (d, $J_{H-H} = 7.8$, 1H, C_9H_6), 7.70 (d, $J_{H-H} = 7.6$, 1H, C_9H_6), 7.62 (t, $J_{H-H} = 7.6$, 1H, C_9H_6), 7.46 (dd, $J_{H-H} = 4.9$, $J_{H-H} = 7.8$, 1H, C_9H_6), 2.08 (s, 3H, -CH_3), 1.81 (m, 6H, PC*H*$(CH_3)_2$), 1.00 (dvt, $N = 12.8$, $J_{H-H} = 6.4$, 18H, PCH(C*H*$_3)_2$), 0.80 (dvt, $N = 13.7$, $J_{H-H} = 6.1$, 18H, PCH(C*H*$_3)_2$), −11.84 (br, 2H, OsH), −17.37 (t, $J_{H-P} = 13.7$, 1H, OsH). $^{31}P\{^1H\}$ NMR (121.42 MHz, CD_2Cl_2 213 K): δ 24.5 (s). $^{13}C\{^1H\}$ NMR (100.56 MHz, CD_2Cl_2, 213 K, plus apt): δ 154.6 (s, C_9H_6), 148.8 (s, C_{ipso} C_9H_6), 138.3 (s, C_9H_6), 134.3 (s, C_9H_6), 131.5 (s, C_9H_6), 130.4 (s, C_{ipso}, C_9H_6), 128.8 (s, C_9H_6), 127.8 (s, C_9H_6), 123.0 (s, C_9H_6), 25.5 (vt, $N = 25.7$, PC*H*$(CH_3)_2$), 19.5, 18.9 (both s, PCH(C*H*$_3)_2$), −10.0 (s, CH_3). $T_{1(min)}$ (ms, OsH, 300 MHz, CD_2Cl_2, 203 K): 31.0 ± 1 (−11.80 ppm), $T_{1(min)}$ (ms, OsH, 300 MHz, CD_2Cl_2, 223 K): 90.8 ± 1 (−17.34 ppm).

Preparation of $[OsH_3\{{=}CHN(CH_3)$-*o*-$C_5H_4N\}(P^iPr_3)_2]BF_4$ (7). A solution of **3** (120 mg, 0.189 mmol) in 20 mL of dichloromethane was treated with 1 equiv of $HBF_4{\cdot}OEt_2$ (25.7 μL, 0.189 mmol) and stirred for 20 min at room temperature. The solution color changed from yellow to orange. The resulting solution was filtered through Celite and concentrated to ca. 0.5 mL. Diethyl ether was added to afford an orange solid, with was also washed with further portions of diethyl ether at 233 K and dried *in vacuo*. Yield: 128 mg (94%). Anal. Calcd for $C_{25}H_{53}BF_4N_2OsP_2$: C, 41.66; H, 7.41; N, 3.88. Found: C, 41.65; H, 7.31; N, 3.98. IR (Nujol, cm^{-1}): ν(OsH) 2022 (s), 2125 (s). ^1H NMR (300 MHz, CD_2Cl_2, 293 K): δ 12.80 (q, $J_{H-H} = 5.0$, 1H, Os=C*H*), 9.26 (d, $J_{H-H} = 7.6$, 1H, py), 7.92 (t, $J_{H-H} = 7.6$, 1H, py), 7.71 (d, $J_{H-H} = 7.6$, 1H, py), 7.18 (t, $J_{H-H} = 7.6$, 1H, py), 3.91 (s, 3H, CH_3), 1.77 (m, 6H, PC*H*$(CH_3)_2$), 1.04 (dvt, $N = 13.7$, $J_{H-H} = 7.0$, 18H, PCH(C*H*$_3)_2$), 0.86 (dvt, $N = 13.9$, $J_{H-H} = 7.1$, 18H, PCH(C*H*$_3)_2$) −8.36 (td, $J_{H-P} = 14.7$, $J_{H-H} = 5.0$, 3H, OsH). $^1H\{^{31}P\}$ NMR (300 MHz, CD_2Cl_2, 183 K, hydride region): ABC part of an $ABCMX_2$ spin system, $\delta_A = -5.0$, $\delta_B = -9.5$, $\delta_C = -11.5$ ($J_{A-B} = 317$, $J_{A-C} = 10$, $J_{B-C} = 400$ Hz, OsH). $^{31}P\{^1H\}$ NMR (121.42 MHz, CD_2Cl_2, 293 K): δ 36.3 (s). $^{13}C\{^1H\}$ NMR (75.42 MHz, CD_2Cl_2, 293 K): δ 248.1 (s, =*C*H), 157.9 (s, py), 156.8 (s, py), 138.5 (s, py), 121.8 (s, py), 114.1 (s, py), 45.9 (s, CH_3), 27.9 (vt, $N = 27.4$, PC*H*$(CH_3)_2$), 19.5, 19.3, (both s, PCH(C*H*$_3)_2$). MS (FAB$^+$): *m*/*z* 634 (M^+).

Structural Analysis of Complexes 6 and 7. Crystals suitable for the X-ray diffraction study were obtained by slow diffusion of diethyl ether into a concentrated solution of the complexes in dichloromethane at −20 °C. X-ray data were collected for both complexes on a Bruker Smart APEX CCD diffractometer equipped with a normal focus, 2.4 kW sealed tube source (Mo radiation, $\lambda = 0.71073$ Å) operating at 50 kV and 30 mA. Data were collected over the complete sphere by a combination of four sets. Each frame exposure time was 10 s covering 0.3° in ω. Data were corrected for absorption by using a multiscan method applied with the SADABS program.[41] The structures of both compounds were solved by the Patterson method. Refinement, by full-matrix least-squares on F^2 with SHELXL97,[42] was similar for all complexes, including isotropic and subsequently anisotropic displacement parameters. For complex **6** the hydride ligands were located, but they do not refine properly, and the Os−H distance was fixed to 1.59(1) Å. The hydrogen atoms of the CH_3 group were located in the difference Fourier maps and refined isotropically. The remaining hydrogen atoms were included in calculated positions and refined riding on their respective carbon atoms with the thermal parameter related to the bonded atoms. The BF_4 anion was observed disordered. The anion was defined with two moieties, complementary occupancy factors, isotropic atoms, and restrained geometry. In complex **7**, several methyl groups of the triisopropylphosphine ligands were refined in two positions (0.5). These groups were refined with an isotropic model and restrained geometry. The hydride ligands were observed in the difference Fourier maps and refined as isotropic atoms with the same distance to the osmium atom (1.59(1) Å). The hydrogen atom of the carbene carbon atom was located and refined isotropically. The remaining hydrogen atoms were included in calculated positions and refined riding on their respective carbon atoms with the thermal parameter related to the bonded atoms. In both complexes, all the highest electronic residuals were observed in close proximity of the Os centers and make no chemical sense. Crystal data and details of the data collection and refinement are given in Table 1.

(41) Blessing, R. H. *Acta Crystallogr.* **1995**, *A51*, 33. *SADABS*, Area-detector absorption correction; Bruker-AXS: Madison, WI, 1996.

(42) *SHELXTL* Package v. 6.10; Bruker-AXS: Madison, WI, 2000. Sheldrick, G. M. *SHELXS-86* and *SHELXL-97*; University of Göttingen: Göttingen, Germany, 1997.

Table 1. Crystal Data and Data Collection and Refinement for 6 and 7

	6	7
	Crystal Data	
formula	$C_{28}H_{54}BF_4NOsP_2$	$C_{25}H_{53}BF_4N_2OsP_2$
molecular wt	743.67	720.64
color and habit	yellow, irregular block	orange, prism
size, mm	0.24 × 0.12 × 0.08	0.16 × 0.14 × 0.12
symmetry, space group	triclinic, $P\bar{1}$	orthorhombic, $P2(1)2(1)2(1)$
a, Å	8.5609(13)	12.0743(17)
b, Å	11.7715(17)	15.241(2)
c, Å	17.222(3)	16.790(2)
α, deg	77.477(2)	90
β, deg	79.399(2)	90
γ, deg	70.940(2)	90
V, Å^3	1589.3(4)	3089.6(8)
Z	2	4
D_{calc}, g cm^{-3}	1.554	1.549
	Data Collection and Refinement	
diffractometer	Bruker Smart APEX	
λ(Mo Kα), Å	0.71073	
monochromator	graphite oriented	
scan type	ω scans	
μ, mm^{-1}	4.154	4.271
2θ, range deg	3, 58	3, 58
temp, K	100.0(2)	100.0(2)
no. of data collect	19 781	39 087
no. of unique data	7584 (R_{int} = 0.0324)	7661 (R_{int} = 0.0483)
no. of params/restraints	359/23	335/29
Flack parameter		0.000(8)
R_1[a] [$F^2 > 2\sigma(F^2)$]	0.0284	0.0350
wR_2[b] [all data]	0.0575	0.0669
S[c] [all data]	0.949	0.927

[a] $R_1(F) = \sum||F_o| - |F_c||/\sum|F_o|$. [b] $wR_2(F^2) = \{\sum[w(F_o^2 - F_c^2)^2]/\sum[w(F_o^2)^2]\}^{1/2}$. [c] Goof = $S = \{\sum[F_o^2 - F_c^2)^2]/(n - p)\}^{1/2}$, where n is the number of reflections and p is the number of refined parameters.

Computational Details. Quantum mechanical calculations were performed with the Gaussian03 package[43] at the DFT B3PW91 level.[44,45] The template of the real system $Os(P^iPr_3)_2$ was simplified to $Os(PMe_3)_2$, in which the isopropyl groups have been substituted by methyl ones. Core electrons of the Os and P atoms were described using the effective core pseudopotentials of Hay−Wadt,[46,47] and valence electrons were described with the standard LANL2DZ basis set.[43] In the case of the P atoms, a set of d-type functions was added.[48] All carbon and hydrogen atoms of the phosphine ligands were described with a 6-31G basis set.[49] The hydrogen atoms directly bonded to the Os center, as well as those susceptible of forming agostic interactions, were described with a 6-31G(d,p) set of basis functions.[49] Carbon and nitrogen atoms bonded to the metal or participating in agostic interactions were described with a 6-31G* basis set.[49] The rest of the atoms in the pyridine-based ligand were described with a 6-31G basis set.[49] Minima and transition states were characterized by analytically computing the Hessian matrix. Information on atom coordinates (*xyz* files) for all optimized structures of minima and transition states is collected in the Supporting Information.

Acknowledgment. Financial support from the MEC of Spain (Projects CTQ2005-00656, CTQ2005-9000-C02-01, and Consolider Ingenio 2010 CSD2007-00006) is gratefully acknowledged. B.E. thanks the Spanish MEC for her grant. M.B. thanks the Spanish MEC/Universidad de Zaragoza for funding through the "Ramón y Cajal" program.

Supporting Information Available: X-ray analysis and crystal structure determinations, including bond lengths and angles of compounds **6** and **7**. Full list of authors for ref 43. Orthogonal coordinates and absolute energies of the optimized theoretical structures. This material is available free of charge via the Internet at http://pubs.acs.org.

OM700509D

(43) Frisch, M. J.; et al. *Gaussian 03*, Revision C.02; Gaussian, Inc., Wallingford, CT, 2004 (for complete reference, see Supporting Information).
(44) Becke, A. D. *J. Chem. Phys.* **1993**, *98*, 5648.
(45) (a) Perdew, J. P. In *Electronic Structure of Solids ' 91*; Ziesche, P., Eschrig, H., Eds.; Akademie Verlag: Berlin, 1991; p 11. (b) Perdew, J. P.; Wang, Y. *Phys. Rev. B* **1992**, *45*, 13244.
(46) Wadt, W. R.; Hay, P. J. *J. Chem. Phys.* **1985**, *82*, 284.
(47) Hay, P. J.; Wadt, W. R. *J. Chem. Phys.* **1985**, *82*, 299.
(48) Höllwarth, A.; Bohme, M.; Dapprich, S.; Ehlers, A.; Gobbi, A.; Jonas, V.; Kohler, K.; Stegmann, R.; Veldkamp, A.; Frenking, G. *Chem. Phys. Lett.* **1993**, *208*, 237.
(49) (a) Ditchfield, R.; Hehre, W. J.; Pople, J. A. *J. Chem. Phys.* **1971**, *54*, 724. (b) Hehre, W. J.; Ditchfield, R.; Pople, J. A. *J. Chem. Phys.* **1972**, *56*, 2257. (c) Hariharan, P. C.; Pople, J. A. *Mol. Phys.* **1974**, *27*, 209. (d) Gordon, M. S. *Chem. Phys. Lett.* **1980**, *76*, 163. (e) Hariharan, P. C.; Pople, J. A. *Theor. Chim. Acta* **1973**, *28*, 213. (f) Blaudeau, J.-P.; McGrath, M. P.; Curtiss, L. A.; Radom, L. *J. Chem. Phys.* **1997**, *107*, 5016. (g) Francl, M. M.; Pietro, W. J.; Hehre, W. J.; Binkley, J. S.; DeFrees, D. J.; Pople, J. A.; Gordon, M. S. *J. Chem. Phys.* **1982**, *77*, 3654. (h) Binning Jr., R. C.; Curtiss, L. A. *J. Comput. Chem.* **1990**, *11*, 1206. (i) Rassolov, V. A.; Pople, J. A.; Ratner, M. A.; Windus, T. L. *J. Chem. Phys.* **1998**, *109*, 1223. (j) Rassolov, V. A.; Ratner, M. A.; Pople, J. A.; Redfern, P. C.; Curtiss, L. A. *J. Comput. Chem.* **2001**, *22*, 976.